THE HANLE EFFECT IN BARIUM

A Thesis

Submitted to

The Faculty of Graduate Studies

University of Manitoba

In Partial Fulfillment

of the Requirements for the Degree of

Doctor of Philosophy

by

Leslie Owen Dickie

Winnipeg Manitoba

March 1971

TABLE OF CONTENTS

ABSTRACT

The lifetime of the 6s6p, 6s7p, and 5d6p $^1P_1$ levels of barium have been determined from the full width at half height of the Hanle resonances of these levels. The resonances were observed using the transitions from the levels to the ground level $6s^2\ ^1S_0$. The oscillator strengths of transitions from the levels have been obtained from the lifetime using the branching ratios given by Penkin and Shabanova (1962) and Ostrovskii and Penkin (1960). Results are;

τ	$6s6p\,^1P_1$	$8.37 \pm 0.14 \times 10^{-9}$ s
τ	$6s7p\,^1P_1$	$13.2 \pm 0.4 \times 10^{-9}$ s
τ	$5d6p\,^1P_1$	$12.22 \pm 0.10 \times 10^{-9}$ s

f(5535)	$6s6p\,^1P_1$	→	$6s^2\ ^1S_0$	1.59 ± 0.1
f(3072)	$6s7p\,^1P_1$	→	$6s^2\ ^1S_0$	0.12 ± 0.05
f(4726)	$6s7p\,^1P_1$	→	$6s5d\,^1D_2$	0.09 ± 0.04
f(3501)	$5d6p\,^1P_1$	→	$6s^2\ ^1S_0$	0.10 ± 0.02
f(5826)	$5d6p\,^1P_1$	→	$6s5d\,^1D_2$	0.19 ± 0.04

Ostrovskii, Yu. I. and Penkin, N.P. 1960, Optics Spectrosc. 9, 371.

Penkin, N.P. and Shabanova, L.M. 1962, Optics Spectrosc. 12, 1.

ACKNOWLEDGEMENT

The assistance of my supervisor Dr. F.M. Kelly is gratefully acknowledged.

LIST OF FIGURES

LIST OF TABLES

CHAPTER I INTRODUCTION

Over the past 100 years optical spectroscopy has provided a great deal of information about atomic structure and in addition has provided important experimental tests of the theory of the atom. Balmer's discovery in 1885 of the relationship between the wavelengths of the series of lines in the hydrogen spectrum that now bears his name can, somewhat arbitrarily, be considered as the beginning of optical spectroscopy.

Shortly after this Zeeman (Zeeman 1897, see Van Heel 1961) published his observation of the effect of a magnetic field on the width of one of the sodium D lines, and, in 1905 Wood (1905) showed that the D lines of sodium could excite D line fluorescence in sodium vapour. Following the discovery of the polarization of the 2537 Å resonance fluorescence of mercury by Rayleigh in 1922, Wood and Ellet (1922) showed that a small magnetic field could change or destroy this polarization, and in 1924 Hanle was able to explain this depolarization of resonance radiation in terms of the Zeeman effect of the excited atomic level. This effect is now called the Hanle effect.

This early work on the Hanle effect, and on resonance radiation in general, is discussed by Mitchell and Zemansky (1934) who describe several Hanle experiments designed to measure the mean lives of excited atomic states and who give still-useful discussions of many experimental details. The early experimenters faced difficulties; for example the intensities of different polarization components could

only be measured photographically or with what would now be rather poor photocells, and the method fell into disuse.

In 1949 Bitter (1949, 1962) suggested that magnetic resonances in optically excited atomic states might be detected optically but his arguments were shown to be false by Pryce (1950). However, shortly after this Brossel and Kastler (1949) suggested that the effects of induced transitions between the sublevels of an excited state might be detected, and the first double resonance experiment was performed by Brossel and Bitter (1952) in 1950. This experiment stimulated much work in optics and many atomic parameters were measured and studied using the double resonance technique.

In 1959 Colgrove, Franken, Lewis, and Sands (1959) accidentally discovered that under certain conditions interference effects between the different polarization components of resonance fluorescence could be observed when two energy levels become degenerate under the influence of a magnetic field. Such level crossing experiments have become important in atomic spectroscopy. The Hanle effect is the special case of a level crossing that occurs when the Zeeman states of a level become degenerate at zero field. Several recent review articles discuss the uses of level crossing, Hanle effect, and double resonance experiments in studying atomic and molecular systems; for example Budick (1967), ZuPutlitz (1965, 1969), Happer (1968), Series (1959, 1969).

Atomic barium has a $6s^2\ {}^1S_0$ ground level. Since J = 0 there is no hyperfine structure in this ground level and to obtain information about the nuclear moments it is necessary to study the hyperfine structure of the excited levels. As well as the interest in an accurate knowledge of the nuclear moments the structure of the excited levels are of interest because small departures from LS coupling lead to small splittings of the ^1P levels whereas none is expected for pure LS coupling. Breit and Wills (1933) have discussed the general theory of hyperfine structure in intermediate coupling while Lurio, Mandl, and Novick (1962) have given the second order hyperfine and Zeeman corrections for an sp configuration while Lurio (1966) had discussed the importance of configuration interaction. The nuclear hyperfine splittings and isotope shifts of many of the barium energy levels are small and give rise to hyperfine structure that is of the same order of magnitude as the room temperature Doppler width of the spectral lines joining the levels. Consequently, if the Doppler width is not reduced by some experimental technique the small hyperfine splittings can not be observed.

The hyperfine shifts between the seven different isotopes are of interest because of the unusual changes that occur as the number of neutrons changes. A number of investigators have studied these shifts using atomic beams, in both emission and absorbtion, to reduce the Doppler width while obtaining the required resolving power with conventional or spherical Fabry-Perot etalons; references

to earlier work are given by Kelly and Tomchuk, (1964), Jackson and Duong (1966) and Fisher and Huhnermann (1969).

Jackson and Duong (1963) also measured the hyperfine structure of the odd isotopes 135 and 137 using high resolution spectroscopy and obtained values for the magnetic and quadrupole coupling constants. The accuracy of their results was quite good even though the structure of the line studied ($6s^2\ ^1So$ - $6s6p\ ^1P_1$, 5535 Å) was poorly resolved despite their use of separated isotopes (to eliminate problems with isotope shifts) and absorbtion by an atomic beam with a high collimation ratio (55:1) to reduce the Doppler effect.

Prior to this work Bucka, Kopfermann, and ZuPutlitz (1961) had obtained the magnetic and quadrupole coupling constants of the $6s6p\ ^3P_1$ configuration of the odd isotopes using the double resonance method at zero magnetic field. A full account of this work appeared in 1963 (ZuPutlitz 1963). The precision of the double resonance method is greater than that of high resolution spectroscopy and this work with barium serves as a typical example of the increase in accuracy that can result from measuring the hyperfine structure directly, rather than measuring the small separations between the components of a spectral line.

The double resonance method was also used by Bucka and Schussler (1961) to measure the g_J value of the $6s6p\ ^1P_1$ level while Bucka and Nagel (1961) used the same method to obtain the lifetime of the $6s6p\ ^3P_1$ level. Hulpke, Paul and Paul (1964)

obtained the lifetime of 6s6p $^1P_1$ level by the phase-shift method, in which the phase shift between modulated resonance radiation incident onto a cell containing scattering atoms, and the resonance fluorescence emitted by the atoms, is measured and can be related to the lifetime of the level.

The first Hanle experiments on the 6s6p $^1P_1$ level were performed by Lurio (1964) who obtained the lifetime of the level and also the magnetic coupling constant $A(^1P_1)$ of the 137 isotope from the position of the level crossing that occurs at about 150 G. These results were extended (Swagel and Lurio 1968) to include a redetermination of the g_J values of the 6s6p ^1P and ^3P levels with greater accuracy than had been achieved in previous work.

As the work described here was completed the results of Ma, Lido and ZuPutlitz (1970)on the second excited ^1P level became available; these authors obtained the lifetime of the level from the Hanle effect, the g_J value from a double resonance experiment, and the nuclear moments of the 135 and 137 isotopes from level crossing experiments.

The study of the energy levels themselves is important, but, in addition,the transitions between the levels are of interest as accurate values of the oscillator strengths of most lines are lacking. Miles and Wiese (1969) have recently critically evaluated the available data and give references to earlier work. Lifetimes obtained from Hanle effect experiments

provide an important test of these earlier results and in fact the whole of Miles and Wiese's results depend on the lifetime of the 6s6p $^1P_1$ level for a reliable translation from relative to absolute oscillator strengths.

The work described here was undertaken to obtain further information about the lifetime of the ^1P levels of barium and the oscillator strengths of transition from these levels. Figure 1 is a partial energy level diagram of barium showing the relevant lines and levels. The spectrum of barium was analysed by Russell and Moore (1955) and term energies have been given by Moore (1958).

Fig.1 Partial energy level diagram of barium showing the lines and levels relevant to this work.

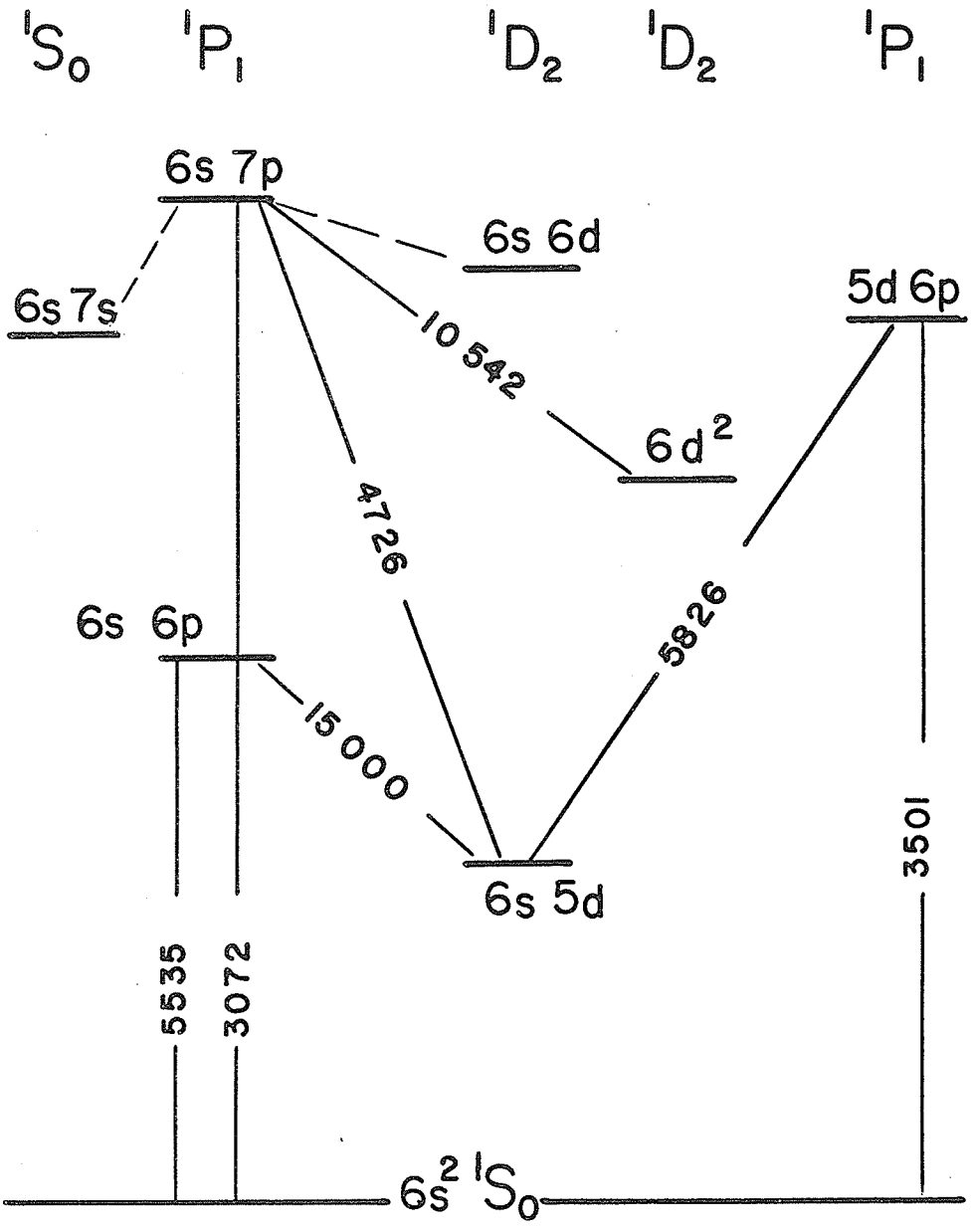
$^1S_0$
$^1P_1$
$^1D_2$
$^1D_2$
$^1P_1$
6s 7p
6s 6d
6s 7s
5d 6p
10 542
$6d^2$
4726
5826
6s 6p
15 000
3501
6s 5d
5535
3072
$6s^2\ ^1S_0$

CHAPTER II EXPERIMENTAL

INTRODUCTION

The general arrangement of the experiment apparatus is shown in Fig. 2. Light from the hollow cathode lamp is focused onto a beam of barium atoms, which is produced by an electrically heated furnace. The resonance radiation scattered from the beam in a direction perpendicular to both the incident light and the magnetic field is collected by a lens and focused onto a photomultiplier. In the early experiments the required line was isolated by an interference filter in each of the input and output light paths, while in later experiments a small grating monochromator in the output light path was used. The light can be plane polarized by polaroid filters. The magnetic field is supplied by sets of Helmholtz coils.

Fig.2 General arrangement of the experimental apparatus.

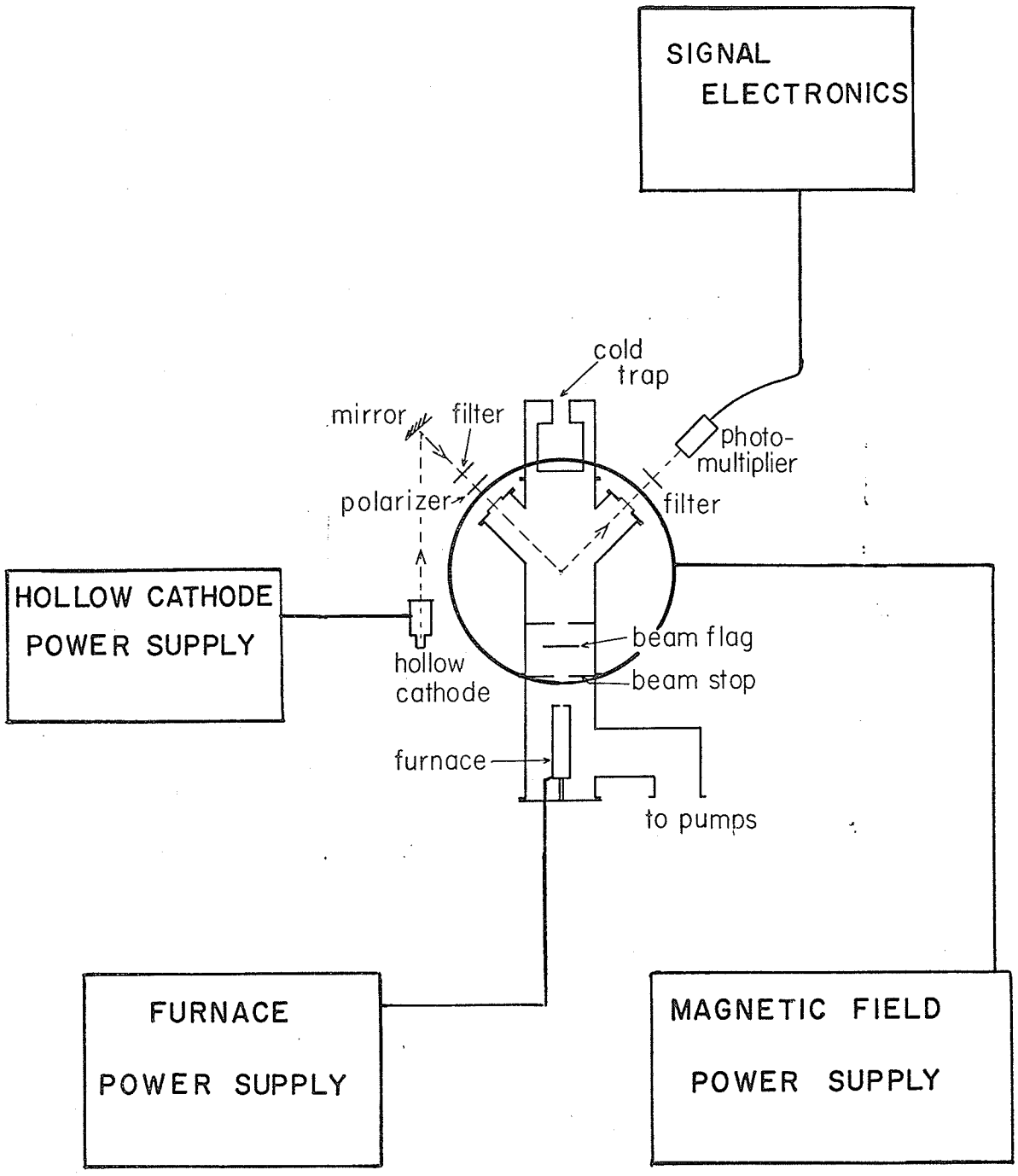
SIGNAL
ELECTRONICS
cold
trap
mirror
filter
photo-
multiplier
polarizer
filter
HOLLOW CATHODE
POWER SUPPLY
beam flag
hollow
cathode
beam stop
furnace
to pumps
FURNACE
POWER SUPPLY
MAGNETIC FIELD
POWER SUPPLY

OPTICAL SYSTEM

The optical system is built up using fused quartz lenses and windows which have sufficiently high transmission down to below the 2700 Å required for the experiments. Polaroid filters are used to polarize the input and output light when this is required. For the ultra-violet lines type HNP'B is used; this polarizer has a transmission of about 15-20% for the allowed component and is usable down to about 2700 Å, below which the transmission falls quickly. For the lines in the visible type HN38 is used; this has a higher transmission, about 40% for the allowed component. Both polaroids transmit less than 1% of the forbidden component . Use of a polarizer improves the signal to noise ratio considerably despite the high absorption and for this reason one is used even though (for a suitable choice of experimental geometry) it is not essential to the observation of the Hanle resonance.

For the experiments with the 5535 Å resonance line an interference filter with a pass band (full width at half intensity of the transmission curve) of about 50 Å, and a peak transmission of about 40%, effectively isolated the line from all other lines emitted by the the lamp. The interference filter used for the 3072 Å experiments had a pass band of about 230 Å and a peak transmission of 25%. After completing these experiments it was found that the lamp was emitting the strong magnesium resonance lines at

2852, 2803, and 2796 Å. These lines were about ten times brighter than the 3072 Å line even after passing through the filter. These lines would not be resonantly scattered by the beam, but they added a constant background to the scattered light and contributed to a poor signal to noise ratio of the 3072 Å experiments. Subsequent experiments using a pure barium cathode in the lamp had a better signal to noise ratio.

For the final experiments a grating monochromator was used to isolate the required lines from the scattered light. The monochromator has a working aperture of f/3.6, its focal length is 0.25 metre, and the pass-band can be set by using different input and output slits.

HOLLOW CATHODE LAMP

The barium resonance radiation is excited in a hollow cathode lamp (Schuler 1926). The design of the lamp used in these experiments is shown in Fig. 3. The lamp is made from two standard conical glass joints and the anode is a thin sheet of aluminium rolled into a hollow cylinder. The cathode is made of copper for good heat conduction. This simple lamp design gives lines of sufficient intensity and is sufficiently stable in operation that the complication of a flow lamp as first used by Cario and Lochte-Holtgreven (1927) and developed by Budick, Novick and Lurio (1965) is not warranted. The discharge is carried by an inert gas (neon) at a pressure of a few mmHg. By bringing the anode close to the cathode so that their separation is less than the length of the dark space the positive column of the discharge is supresssed, and the negative glow is confined to the hollow of the cathode. The ion bombardment and sputtering action of the carrier gas produces the first and second spectra of the cathode material as well as its own spectrum. The pressure of the carrier gas is monitored with a discharge gauge as precise control is not required. The gas handling system is shown schematically in Figure 4. A circulating system (Tolansky 1947) is not used but a liquid nitrogen cooled charcoal trap is used to clean the discharge, in particular to absorb hydrocarbons introduced by the barium, which is stored under kerosene. Initially a magnesium cathode with a small charge of barium was used; the action of the discharge coats the interior of the hollow with barium and magnesium does

Fig.3 Hollow cathode lamp.

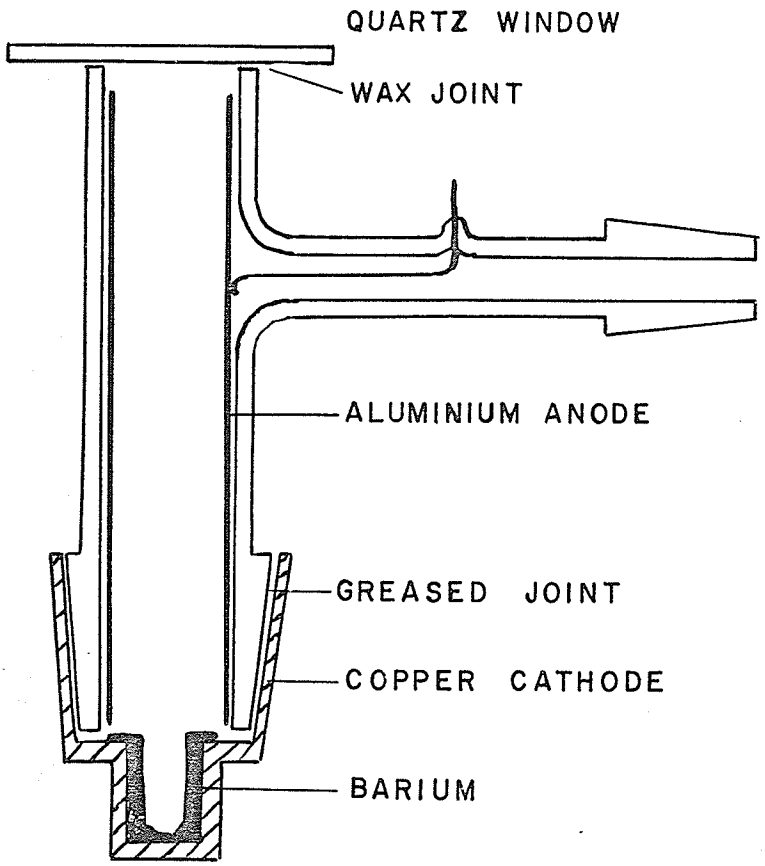
QUARTZ WINDOW
WAX JOINT
ALUMINIUM ANODE
GREASED JOINT
COPPER CATHODE
BARIUM

Fig.4 Gas handling system for the hollow cathode lamp.

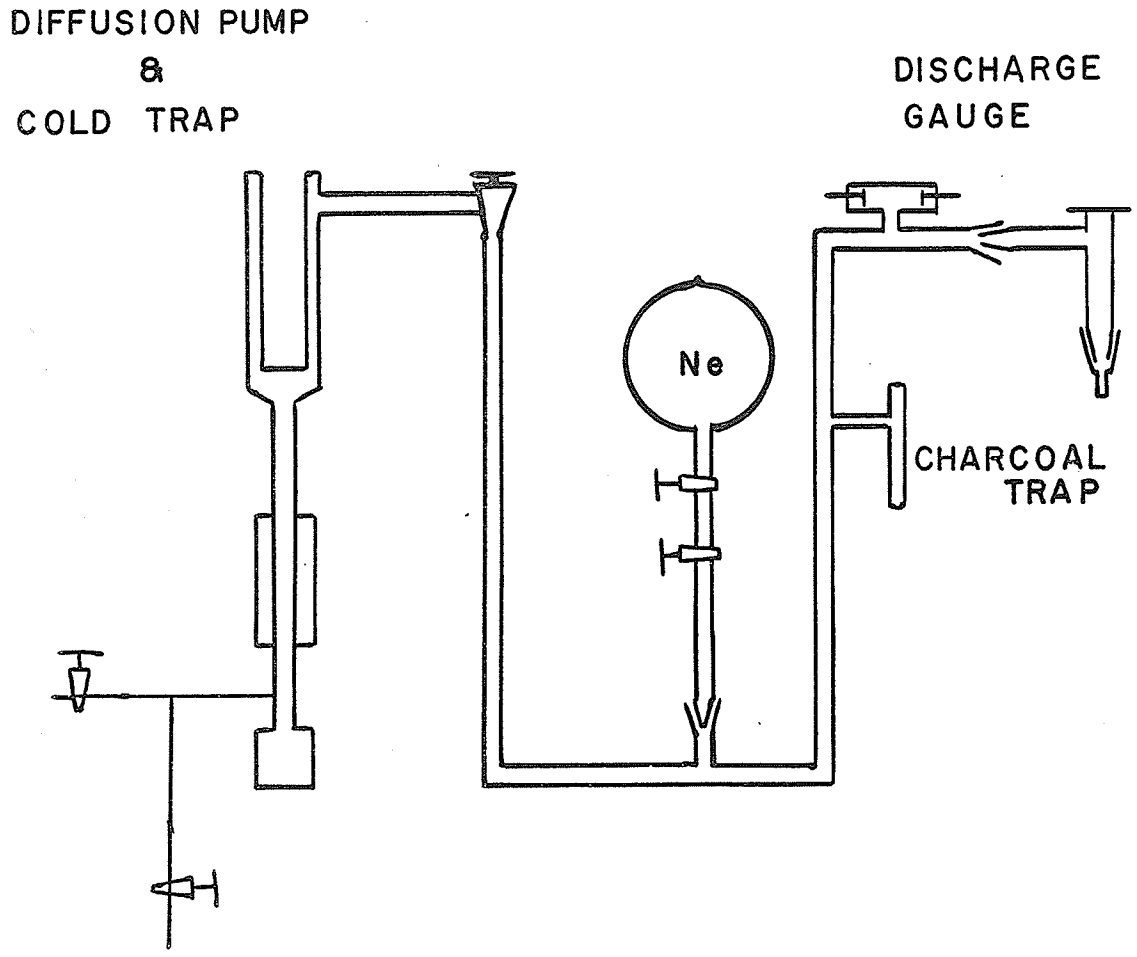
DIFFUSION PUMP
&
COLD TRAP
DISCHARGE
GAUGE
Ne
CHARCOAL
TRAP

not sputter readily. However, it was found that the magnesium I and II resonance lines at 2852, 2803 and 2796 Å were strongly excited and interfered with the experiments on the ultra-violet barium lines at 3072 and 2785 Å. For this reason the magnesium liner of the cathode was removed, a short rod of barium forced into the copper cathode, and a hole drilled in the barium to form the hollow. The dimensions of the hole are 3/8" dia. by 3/4" deep in one lamp and 1/4" by 3/4" in another.

The spectra from the lamps recorded with the experimental apparatus shown in Fig. 5 are shown in Fig. 6.

The theory of the hollow cathode lamp has been discussed by Sawyer (1930), and by Gotmeister (1968); different designs have been given by Tolansky (1947), Arroe and Mack (1950) and Budick et al (1968).

The current in the lamp is controlled by a simple power supply; the output from a variac is rectified, smoothed, then passed through a ballast resistor in series with the lamp. The ballast resistor is necessary to protect the circuit from the negative-resistance characteristics of the lamp as the discharge strikes. Discharge currents between 100 and 300 mA are used.

The light output from the lamp is stable once an initial warm-up period has passed. For the first part of the

Fig.5 Apparatus used to record the spectrum of the hollow cathode lamp.

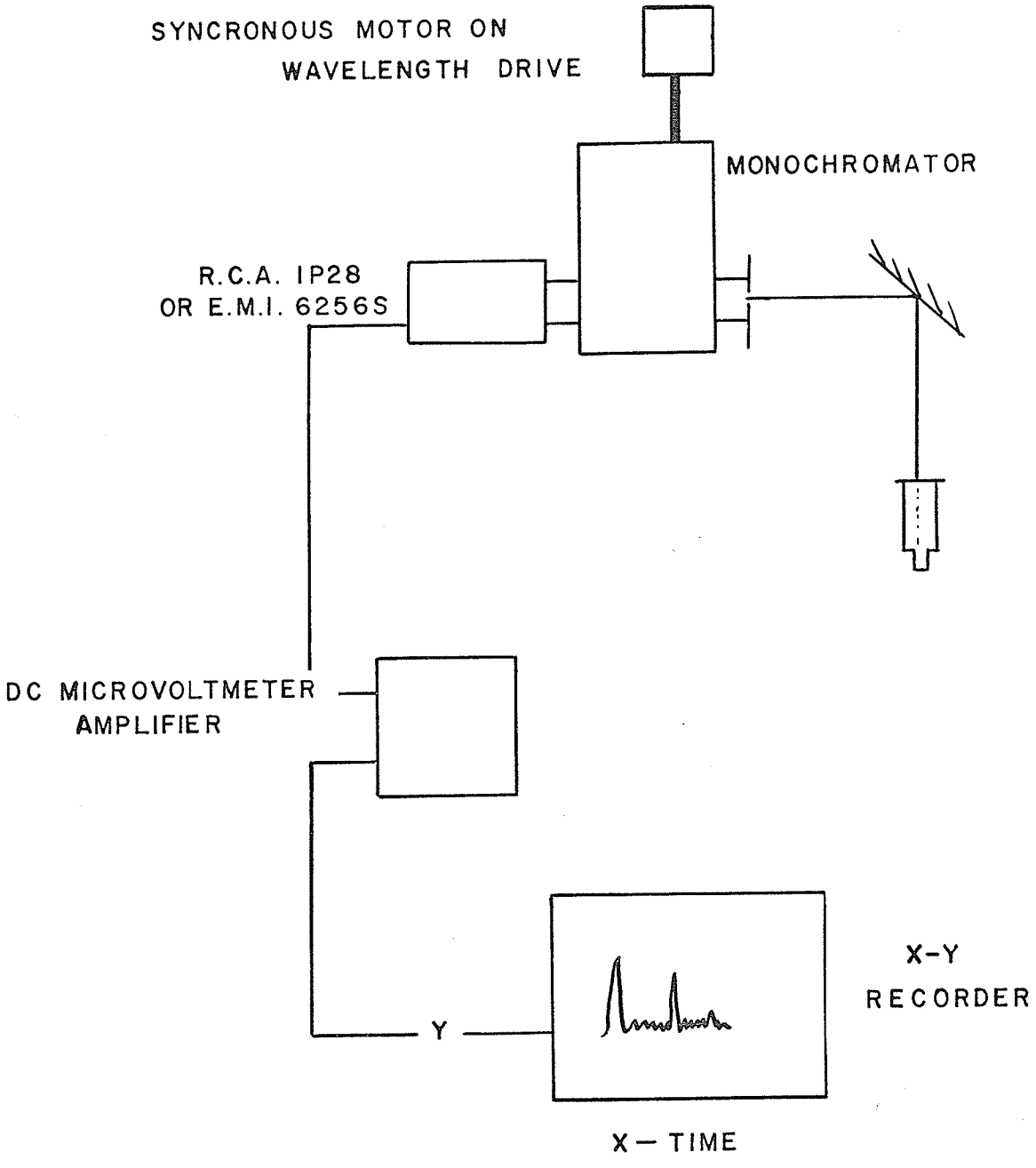
SYNCRONOUS MOTOR ON
WAVELENGTH DRIVE
MONOCHROMATOR
R.C.A. IP28
OR E.M.I. 6256S
DC MICROVOLTMETER
AMPLIFIER
Y
X-Y
RECORDER
X — TIME

Fig.6 Spectrum of the hollow cathode lamp.

(i) red trace; lamp with magnesium liner and a charge of barium.

blue trace; neon lamp with glass envelope.

(ii) lamp with barium cathode.

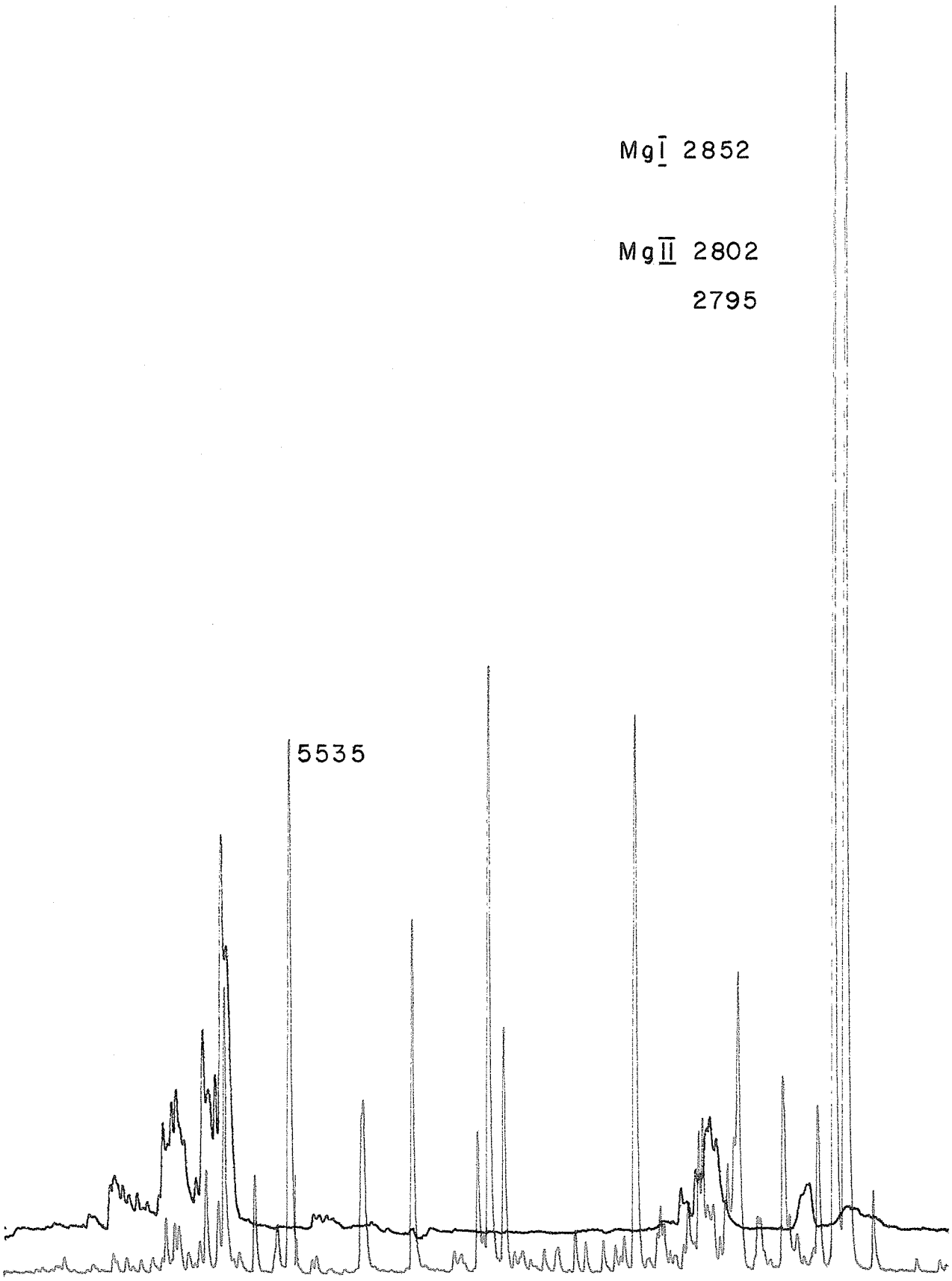
Mg I 2852
Mg II 2802
2795
5535

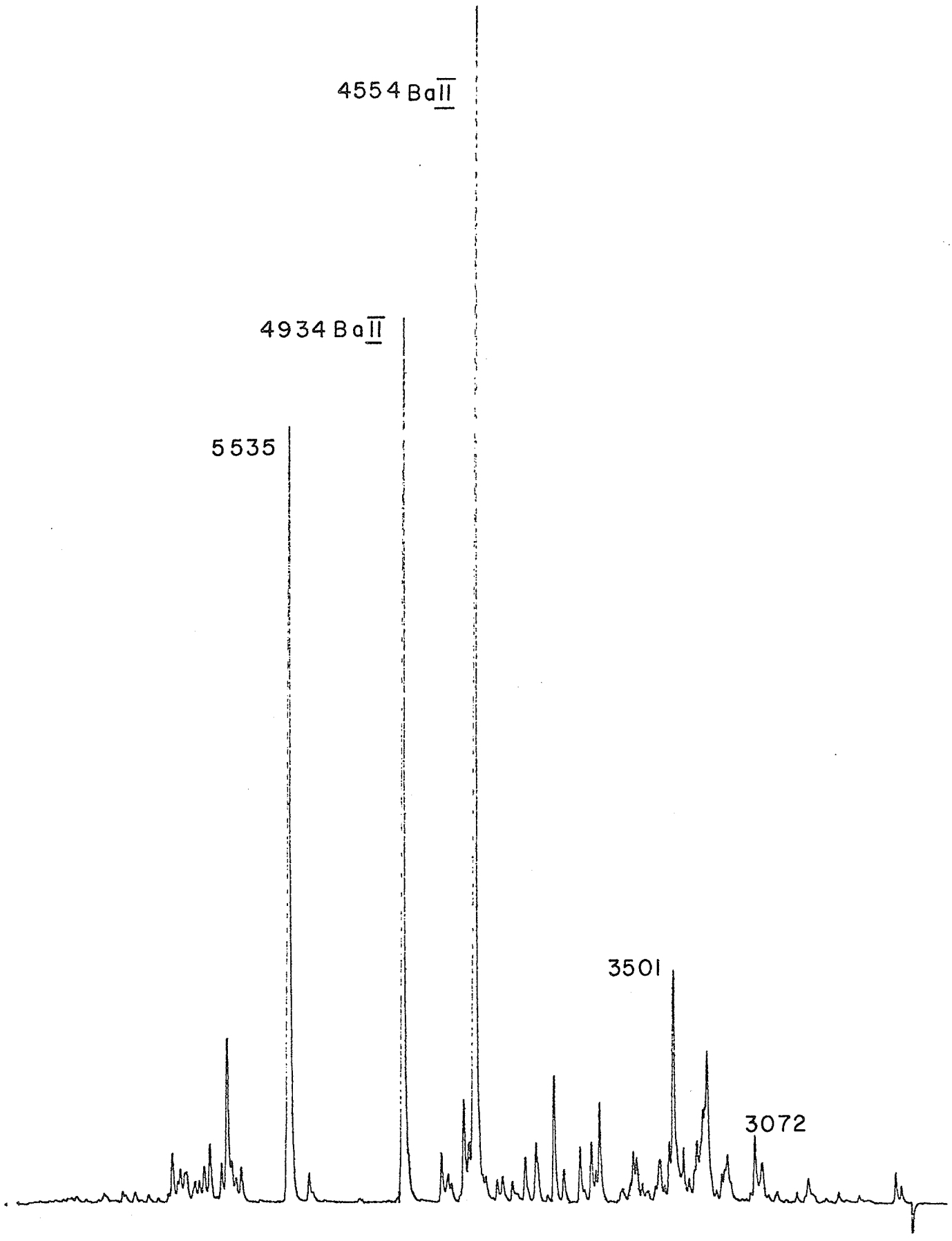
4554 Ba II
4934 Ba II
5535
3501
3072

work it was necessary to ensure that the light output remained constant for periods of 10 minutes or more. It was found that a current controller to maintain a constant discharge current in the lamp was sufficient. The lamp is cooled by an ice-water bath. Typical operating conditions are: voltage drop across the lamp 250V, discharge current 100mA.

VACUUM CHAMBER

The design of the vacuum chamber as shown in Fig. 7 was chosen for the following reasons:

(1) The geometry of the input and output light paths is such that the apparatus can, if required, be placed between the poles of a 5" electromagnet.

(2) The furnace has to be replaced frequently and it is convenient to be able to do this without dismantling the whole apparatus. In addition the furnace tends to shed part of its insulation in use and it is desirable that this not fall into the diffusion pump.

The windows that allow light to enter and leave the vacuum chamber must be shielded from the barium beam because barium attacks quartz rendering it opaque. Randomly scattered light must also be prevented from reaching the output window. A fault in the design is that light from the furnace (usually red hot) is easily scattered into the light input and output arms; it would be better if both of these were at 45^{o} below the horizontal rather than 45^{o} above.

Fig.7 Vacuum chamber.

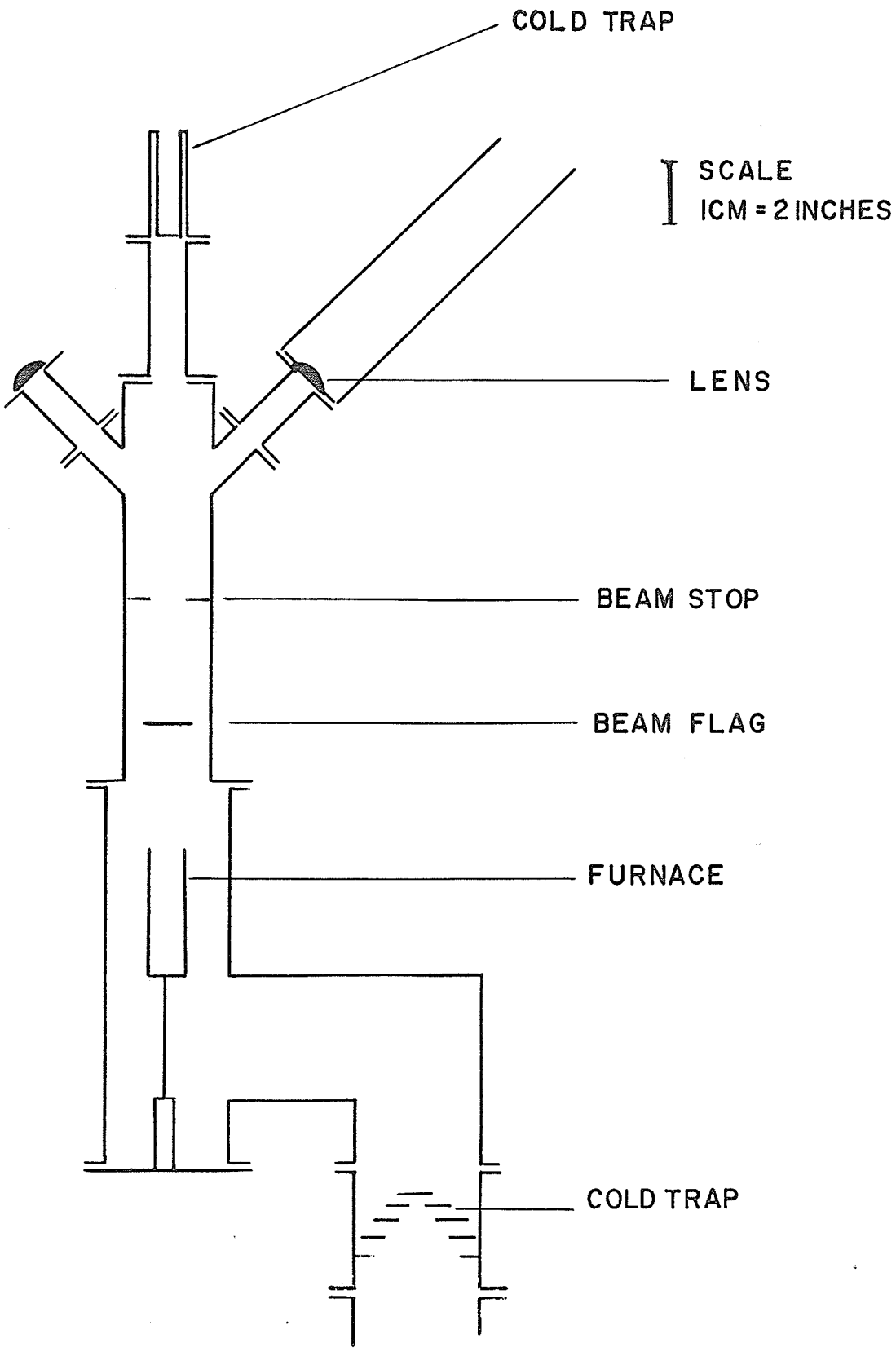
COLD TRAP
SCALE
ICM = 2 INCHES
LENS
BEAM STOP
BEAM FLAG
FURNACE
COLD TRAP

The vacuum chamber or beam tube is made from sections of brass tubing with hard solder on the permanent joints and O-rings sealing the demountable joints. Brass was chosen because it is non-magnetic and the vacuum requirements are not severe. The windows were sealed onto the vacuum chamber with O-rings. Beam stops in the beam tube collimate the beam and help prevent barium reaching the windows. The diameter of the beam at the scattering region is about 1 cm and after passing the scattering region the beam is condensed onto a liquid nitrogen cooled trap or is allowed to condense on a blank flange that can replace the trap.

Diaphragms in the input and output arms help reduce stray scattered light. The chamber is evacuated by a 4" oil diffusion pump backed by a two stage rotary pump. With the beam operating the residual gas pressure in the chamber is about 10^{-5} mmHg. The gettering action of the evaporated barium helps offset the outgasing of the furnace. The oil in the diffusion pump becomes contaminated quite quickly and must be replaced frequently.

FURNACE

The final design of the furnace and its support is shown in Fig. 8. The body of the furnace is made from a 1" diameter stainless steel rod with a 7/8" hole bored into it (the diameter of the barium rods is 3/4"). The furnace is coated with a thin layer of boron nitride (carborundum type S)

Fig.8 Furnace and support.

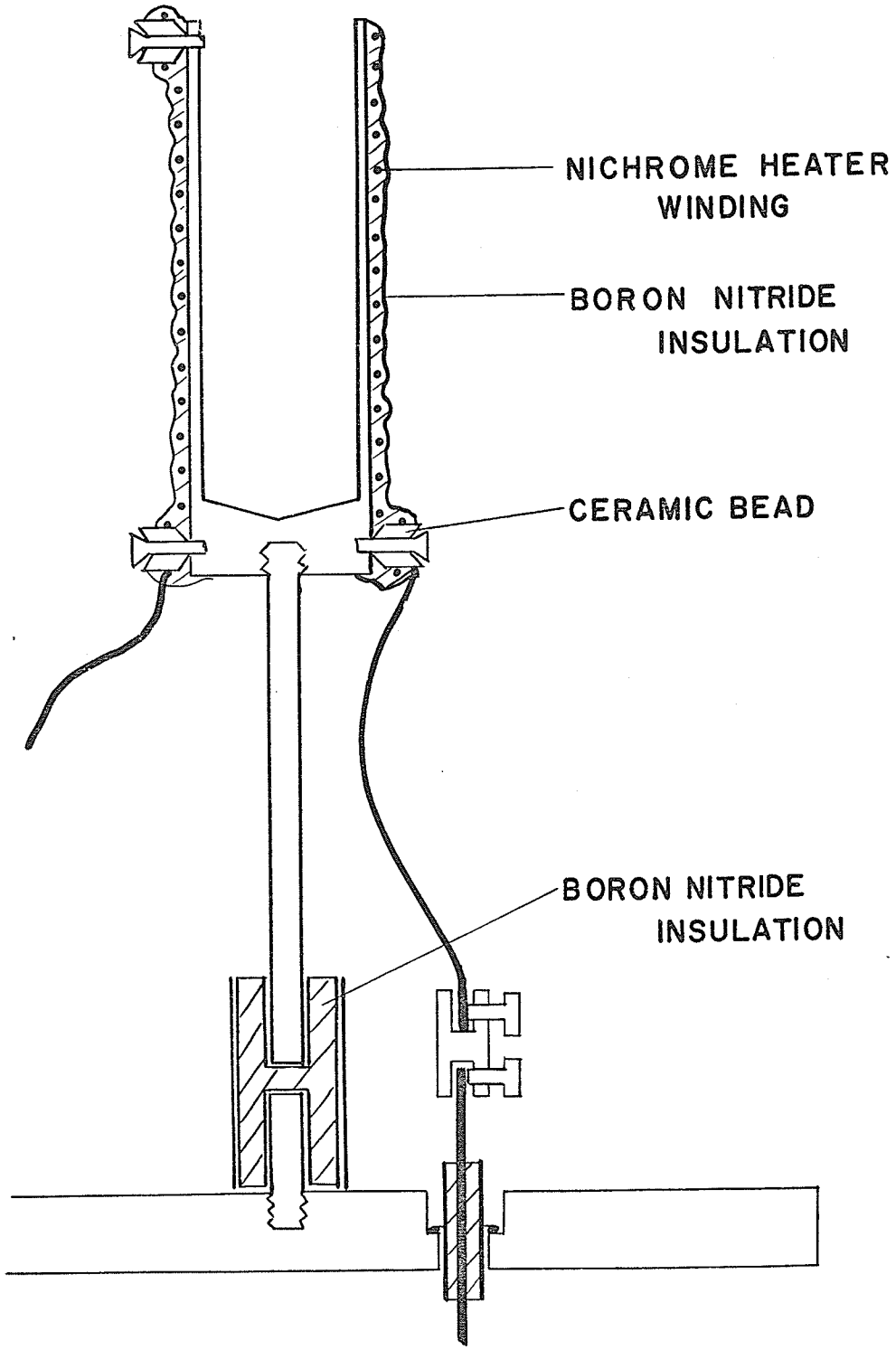
NICHROME HEATER WINDING
BORON NITRIDE INSULATION
CERAMIC BEAD
BORON NITRIDE INSULATION

and a bifilar spiral of nichrome wound onto it. The ends of the winding are secured by wrapping them around screws insulated with ceramic beads. A coating of boron nitride about 1/2 mm thick is then applied to insulate and secure the winding.

It was found easiest to apply the boron nitride coating when the furnace was hot: for the first coat this was done by heating the furnace with a propane gas torch and for the second coat by passing a current through the winding. The temperature was kept a little above 100°C so that the water in the coating evaporated quickly leaving a thin uniform layer to which another layer could be applied. If several layers were applied without throughly drying each one, all layers quickly flaked off.

The furnace had a useful life of several days at operating temperatures - dull red heat or about 600°C - and was used until the charge of barium was exhausted or the winding burned out. In use the barium tends to penetrate the boron nitride and attack the winding and so contribute to furnace failure.

The bifilar winding is used to reduce stray magnetic fields. Initially the power for the furnace was controlled from the mains by a variac; subsequently a dc supply was built. This supply consists of a variac, full wave rectifer, and some smoothing. Typical operating conditions are: voltage drop across the furnace 35V, current 12A. This amount of power (circa 400 watts) gives a fairly dense beam of barium atoms.

This beam density was used during experiments using the final signal averaging electronics when the lines 3072 and 3501 Å were being studied. Smaller power dissipation gave an adequate signal for the stronger 5535 Å line and the final electronic arrangement. The coherence narrowing of 5535 Å indicates that the highest density of the atomic beam was about 10^{10} atoms per cm^3.

MAGNETIC FIELD

The steady magnetic field at the scattering region is supplied by a pair of Helmholtz coils 40cm in diameter; the coils are wound from copper strips. The coils were adjusted to give a field uniform to one part in 5000 over a cube of side 1". During the adjustments the field was measured with a Rawson-Lush rotating coil gaussmeter whose absolute accuracy is 0.01% but whose differential sensitivity can be much greater than this. The current in the Helmholtz coils is monitored by measuring the voltage across standard 0.1 or 1.0 ohm resistors in series with the coils with a digital voltmeter accurate to 0.02%. The resistor is immersed in an oil bath; the oil in the bath is stirred and the power dissipated in the resistors is small enough that heating the oil and consequent changes in resistance can be neglected.

The gaussmeter was also used to obtain the current-field relationship of the coils. Data from a typical calibration run is given in Table I; the current field relation is essentially linear over the range tested.

In addition to the main set of Helmholtz coils there are three more sets of coils surrounding the scattering region. Two of these sets of coils are used to cancel the two components of the earth's field perpendicular to the field of the main coils. The appropriate currents for these coils were determined

TABLE I

Calibration of Helmholtz Coils	
Volts across 0.1Ω	Field (Gauss)
+0.8006	+248.502
0.7006	217.439
0.6003	186.326
0.5001	155.232
0.4006	124.314
0.3009	93.361
0.2002	62.117
-0.2022	- 62.753
-0.3007	- 93.349
-0.4005	-124.306
-0.5005	-155.359
-0.6004	-186.436
-0.7004	-217.446

Least squaresfit to a straight line gives:-

slope 31.0409 ± 0.003 G/A
constant -0.0191 ± 0.002 G

to take account of uncertainties in the Gauss meter and in the voltmeter multiply variance by two to give calibration of coils

31.040 ± 0.006 G/A

by using a dip needle to determine the (straight-line) relation between the residual field direction and the current in the coils over a range of a few gauss about zero net field. The final set of coils is concentric with the main Helmholtz pair and has a diameter of 30 cm; these coils supply a sweep field to the scattering region. This variable field is used to magnetically scan the system through the resonances. The coils give about 18.736 G/A.

It is difficult to construct a power supply that will pass through zero current without some crossover distortion at zero. Instead, the field of the main coils was set at -60G and the field of the sweep coils varied from 0 to 120G giving a net range of -60 to + 60G. The variation with time is a symmetic triangular ramp with a period of about 1/2 , 1, 2, or 4 seconds. The field over the scattering region must be sufficiently uniform that the band-width due to the inhomogeneities is less than the natural width of the levels being studied.

Taking the lifetime of the levels as 10^{-9} seconds, and using the Heisenberg relation

$$\Delta E \cdot \Delta t \doteqdot \tau$$

and the shift in energy due to the Zeeman effect

$$\Delta E_z = g_J \mu_o m_J \Delta H$$

then for $g_J = 1$, $m_J = 1$ the field in-homogeneities must be smaller than about 10^{-2}G.

SIGNAL ANALYSIS

Experimentally the problem is to obtain the shape of the Hanle resonance. This is obtained as a plot of the scattered light intensity against magnetic field. Two sets of electronics were used to do this; the schematic layouts of these are shown in Fig. 9.

In both methods the resonance radiation scattered from the beam is focused onto an EMI 6256 B photomultiplier. Single photon pulses from the photomultiplier are amplified, then passed to a single channel analyser used either to isolate the single photon peak or, more usually, to discriminate against low energy noise pulses.

In the first method (Fig. 9 (i)) the output from the single channel analyser is fed into a scalar. The shape of the resonance is found by plotting the number of photons scattered into the photomultiplier in a fixed period against the magnetic field. The field is varied in steps from about -60G, through zero, to +60G. A typical run contains between 60 and 100 points. The counting periods at each step are made long enough to give good statistics and are between 1 and 10 seconds; it requires about 10 minutes to accumulate the data.

Fig.9 Signal electronics

(i) photon counting electronics.

(ii) signal averaging electronics.

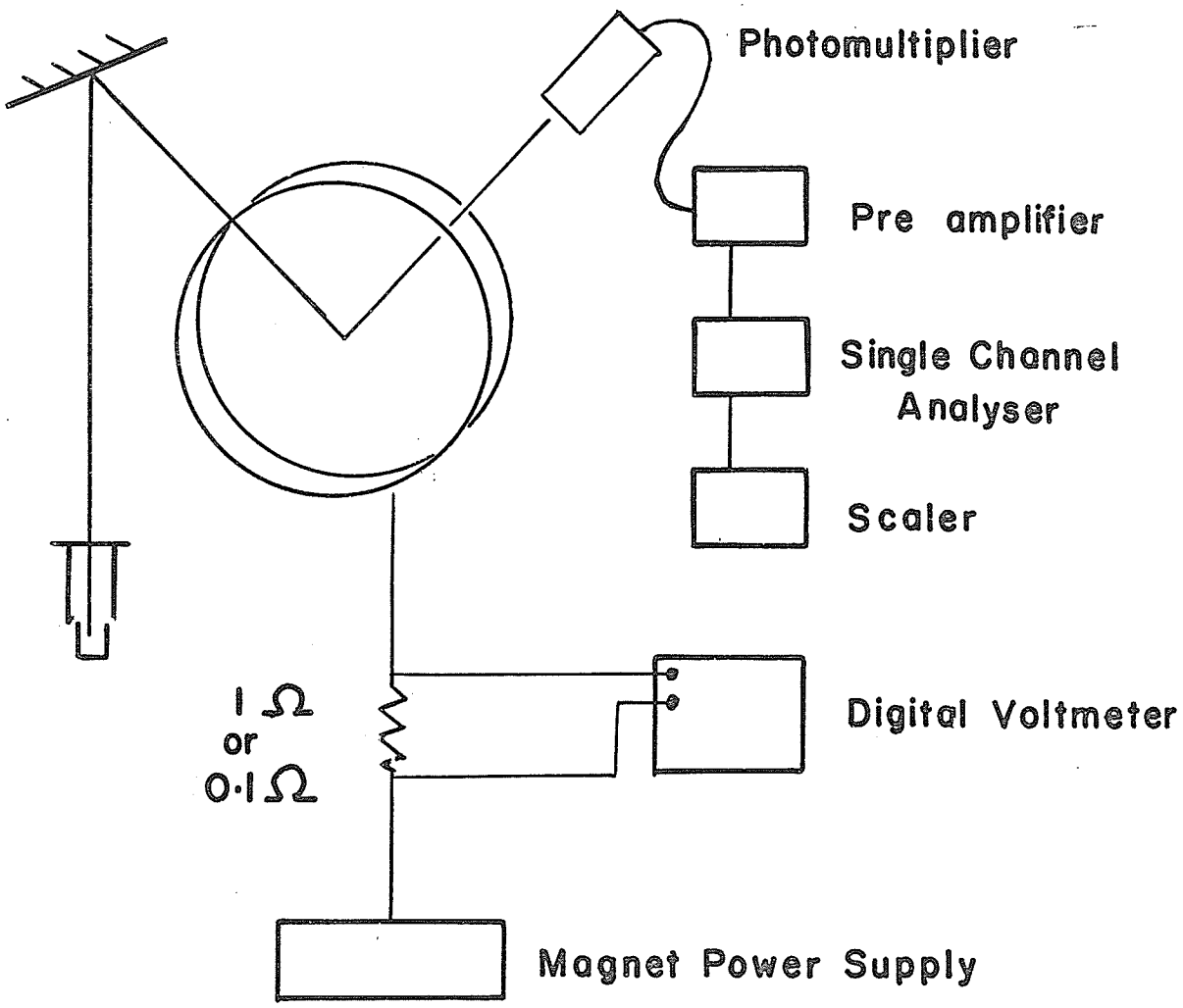
Photomultiplier
Pre amplifier
Single Channel Analyser
Scaler
1 Ω or 0·1 Ω
Digital Voltmeter
Magnet Power Supply

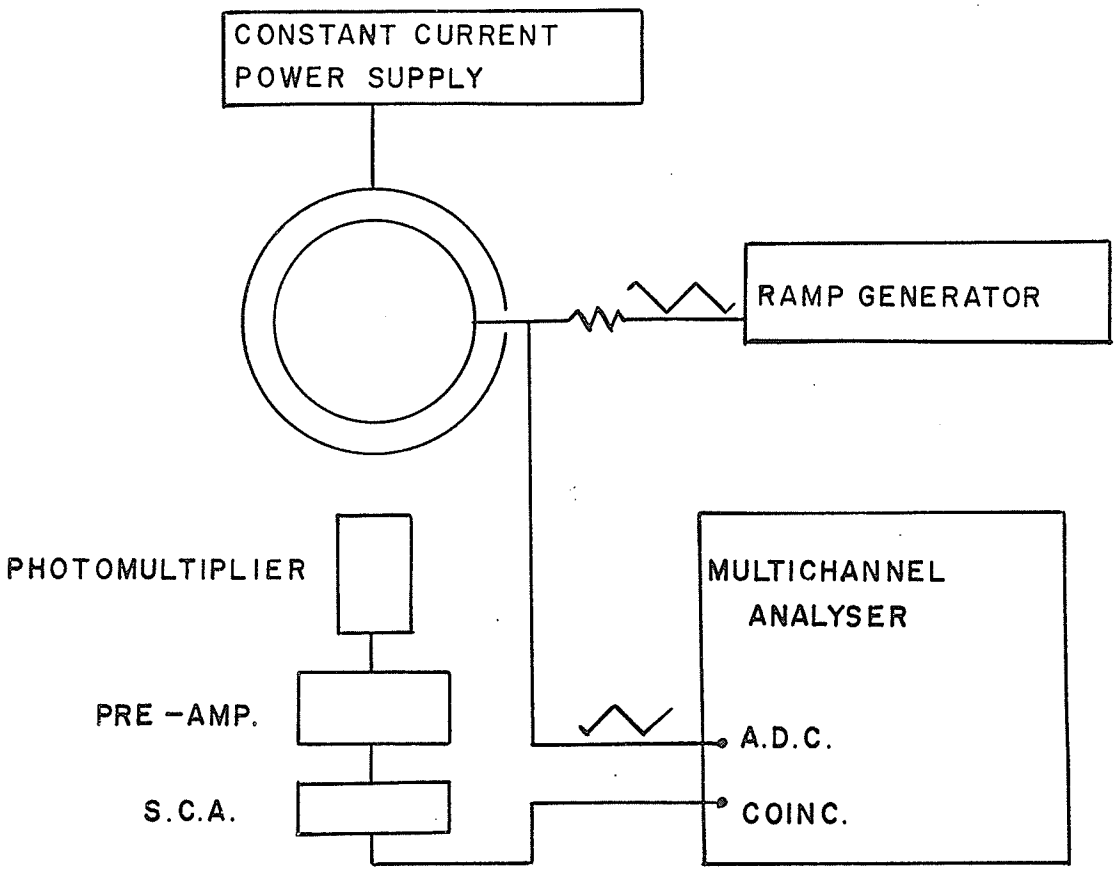
CONSTANT CURRENT
POWER SUPPLY
RAMP GENERATOR
PHOTOMULTIPLIER
PRE-AMP.
S.C.A.
MULTICHANNEL
ANALYSER
A.D.C.
COINC.

The light output from the hollow cathode could be kept constant for this period of time, but difficulties were experienced with gradual changes of the beam density. Since both coherence narrowing and the magnitude of the scattered signal, depend on beam density, only the data that showed a change in signal intensity of a few percent, as reflected by a sloping baseline was used in the analysis.

The second experimental set-up was used to overcome the difficulty of changing beam density and also to increase the signal to noise ratio.

One method of extracting information from noise is to use a lock-in amplifer. There are several objections to this. On what might be called philisophical grounds, there is the objection that it does not seem sensible to convert the single-photon pulses given by the photomultiplier to a dc signal rather than use some technique that directly counts the pulses. In addition it is necessary to supply an oscillating magnetic field to the scattering region if magnetic scanning is used. If the oscillating field has a large amplitude the distortion of the line shape this introduces must be allowed for. Alternatively, if a small oscillating field is used to avoid distortion the phase-syncronous signal is smaller.

To avoid the problems of a lock-in amplier the signal averaging electronics shown in Fig. 9 (ii) were assembled. Using this apparatus the system is magnetically scanned through the

resonance in a time that is long enough that the shape of the resonance is not affected and yet short enough that changes in beam density are negligible and many sweeps can be made in a convenient length of time. By adding the signals from subsequent sweeps the random noise pulses tend to average to a uniform baseline on which the resonant signal appears with its signal to noise ratio improved relative to that of a single sweep. If N sweeps are made the signal to noise ratio is multiplied by $\sqrt{N}$.

The time to sweep the magnetic field was a few seconds while the counts were averaged over periods of a few minutes to a few hours. The information from each sweep is stored in a multichannel analyzer; this is less expensive than a signal averager proper, but has the disadvantage that the size of the numbers making up the data increases constantly. The photon pulses from the single channel analyzer are fed into the coincidence imput of the analyzer, the address of which is controlled by the magnetic field. The voltage across a standard resistor in series with the ramp coils is applied to the direct input of the analogue to the digital converter of the analyser. A photon pulse arriving at the coincidence input causes the analyser to sample the voltage on the direct input and store the count in the appropriate channel. The standard resistor is immersed in an oil bath, which is in turn in an ice-water bath to avoid change in resistance with temperature. Because the count rate at the Hanle peak is different to that in the wings of the resonance the count rate is kept low to ensure that the dead-time

of the analyser is not important.

Rather than detect the change in signal size - or shape - that occurs when the applied magnetic field is changed the change in signal size with changing polarizer angle can also be detected and used to improve the signal to noise ratio. The geometries used for the experiments described in this work are given in Fig. 11. If the output linear polarizer of Fig. 11 (iii) is oriented along the Y axis the output signal as a function of magnetic field is a Lorentzian with the positive peak at zero field. If the polarizer is oriented along the X axis the output signal is an inverted Lorentzian. If the polarizer rotates with angular frequency ω the output signal will swing from plus to minus with frequency 2ω and this signal can be detected with a phase sensitive detector. The same principle can also be used with the geometry shown in Fig. 11 (ii) but here the signal changes from the base-line to the inverted Lorentzian peak as the polarizer angle changes so the synchronous signal produced by rotating the polarizer is correspondingly smaller. Use of a rotating polarizer to produce a synchronous signal is discussed by Handrick et al (1969).

The data given by the multichannel analyser is a plot of light intensity against channel number rather than against magnetic field and the full width of the Hanle resonance must be converted from a number of channels to a magnetic field strength in Gauss. As the field of the ramp coils varies from

0 → 120G the analyser adds counts to channels 1 through 512. The field at the scattering region is the sum of the field of the ramp coils and the steady field of the main Helmholtz coils. The calibration of the main coils is known. By varying the current in the main coils the zero field point can be made to occur anywhere in the 512 channels of the analyser. Using the 5535 Å line, Hanle resonances were obtained with the position of the peak (zero field) at a number of different channel numbers. Suitable curves could be obtained in a few minutes, and the results are given in Table II. Because only the width of the resonance is required an absolute calibration is not necessary and only the slope of the channel number to gauss relation is needed. The points in the table were fitted to a straight line using the method of least squares.

From both methods of collecting the data one obtains a plot of the intensity of the scattered light against magnetic field.

The direct method gives about 60 to 100 points while the signal averaging method gives up to 512, and typically 300 points.

In both cases the data is fitted to a Lorentzian by a computer program run on the University of Manitoba I.B.M. system 360. The program gives the full width at half intensity and other parameters of the best fit, and allows for a sloping baseline to the data. In addition the program plots

TABLE II

Calibration of Multichannel Analyser

Volts across 0.1Ω in series with main coils	Channel number of center of Hanle resonance (from fitting program)
0.0834	108.51
0.1428	180.65
0.2004	250.39
0.2600	320.84
0.3174	389.44

slope of line 0.000 833 53 ± 0.000 000 1

calibration of main Helmholtz coils 31.037 ± 0.006 G/A

conversion factor 0.258 70 ± 0.000 05 G/ch.

on the line printer, a graph of the theoretical and experimental counts against the magnetic field. This plot allows a visual check against gross errors in the program, and gives some indication of the scatter of the experimental points and the symmetry of the fit. The program also plots a graph of the difference between the experimental and theoretical points against magnetic field. This plot is used to check on any systematic errors in the data, and particularly to check whether any dispersive component is present.

CHAPTER III THEORY

INTRODUCTION

When an atom is placed in a magnetic field the energy levels are split into the various Zeeman states. The Zeeman states of any level are degenerate at zero magnetic field. If fine or hyperfine structure is present there is the possibility of two states of different levels crossing, and becoming degenerate, at a non-zero magnetic field. When resonance radiation is scattered from such a system there can be a spatial redistribution of the scattered light at these degeneracies. These resonances can be observed if one component of the resonance fluorescence is monitored as the system is swept through the degeneracy.

When the coupling between the two crossing states is due only to the external perturbation (in this case the magnetic field) the degeneracy is called a level crossing. When there is some internal interaction between the two states, the degeneracy is called an anti-level crossing because the internal coupling will prevent the two states from actually crossing.

In order to observe the level crossing, light in one eigenstate of polarization must be capable of stimulating transitions from some initial state to both of the two crossing states. In addition, these two states must be able to decay

to some common final state, not necessarily the initial state - as shown in Fig. 10.

The effect is similar to a two slit interference experiment in that there are two paths for the atom to follow in going from the initial to the final state and the interference effects this introduces lead to a redistribution of the scattered radiation.

The width of an energy level is inversely proportional to the lifetime of the level. Consequently level crossings of Zeeman states take place over a range of magnetic field and the width of the observed resonance, measured in terms of the magnetic field, depends on the lifetime of the level.

THEORY OF THE HANLE EFFECT

Many features of the interaction of radiation with an atom can be successfully explained in a classical or semi-classical manner (see for example Franken 1969). For the Hanle effect, Happer (1968) has pointed out that quantum mechanics is necessary only if hyperfine structure is present or when two or more fine-structure multiplets are nearly degenerate.

The geometry of the experiments discussed in this work is shown in Fig. 11. A dipole, considered as a classical damped oscillator, at the origin of the coordinate system is

Fig.10 Energy level diagram pertaining to a level crossing experiment.

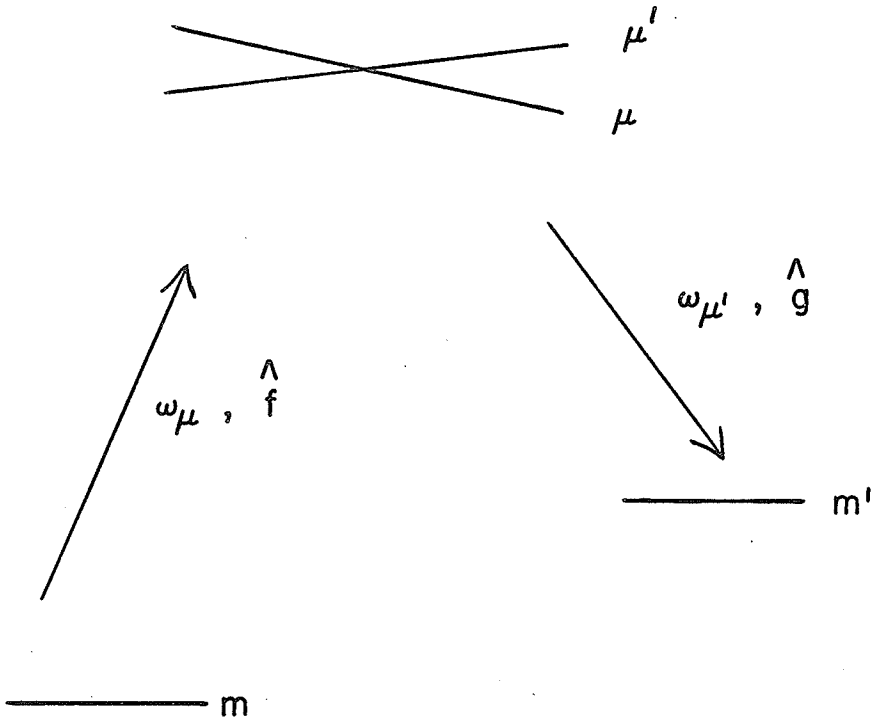
μ'
μ
$\omega_{\mu'}$, $\hat{g}$
ω_{μ} , $\hat{f}$
m'
m

excited by plane polarized light incident along the X axis, with the electric vector of the light in the X-Y plane (Fig. 11 (ii)). In the absence of an external magnetic field the dipole oscillates along the Y axis and no light is emitted along the Y axis. In the presence of a magnetic field in the Z direction the dipole will rotate with the Lamor precession $\omega_L = g_J \mu_o H/h$, about the Z axis. Then, there will be some component of the dipole perpendicular to the Y direction and light will be emitted in the direction of the Y axis.

If the field is strong enough to rotate the dipole several times before its energy is dissipated then the emitted light will be depolarized. A rapidly damped oscillator, i.e. one with a short lifetime, will require a larger field to depolarize the radiation than a more slowly damped one. The width of the Hanle signal will thus be proportional to the reciprocal of the lifetime, and the classical model can be used to predict the relation between the two.

Hanle (1924) was the first to give a theoretical explanation, based on the Zeeman effect, of the depolarization of resonance radiation arising from this zero field level crossing, or, as it is now known, the Hanle effect.

The general theory of the scattering of resonance radiation was developed by Weisskopf (1931) and by Breit (1933) in his review article 'Quantum Theory of Dispersion' in which

level crossing theory is given implicity. More recently the theory has been put into forms more directly useful for atomic spectroscopy by a number of authors, in particular by Franken (1961), and by Rose and Carovillano (1961), while deZafra and Kirk (1967) have given a simplified discussion.

The interaction of resonance radiation with an atom can be conveniently developed by treating the radiation field semi-classically (see for example Heitler 1954). Following the references cited above we can apply time dependent perturbation theory to a system made up of a sample atom and resonance radiation produced by the decay of a source atom. The rate at which radiation is absorbed and re-emitted -- i.e. scattered -- as the excited energy levels are made to cross can then be found.

In fig. II we consider the sample atom at the origin of the co-ordinate system. The state of the atom is represented by the ket $|p\rangle$ where p labels the magnetic quantum number of the Zeeman state. Initially the sample atom is in the ground state m, while the source atom is in an excited state μ. For times $t < 0$ the wave function of the sample atom is

$$|\Psi\rangle = |m\rangle$$

Fig.11 Geometry of the Hanle experiments.

(i) general case.

(ii) geometry used for experiments on the 6s6p and 6s7p ^1P levels

(iii) geometry used for experiments on the 5d6p ^1P level.

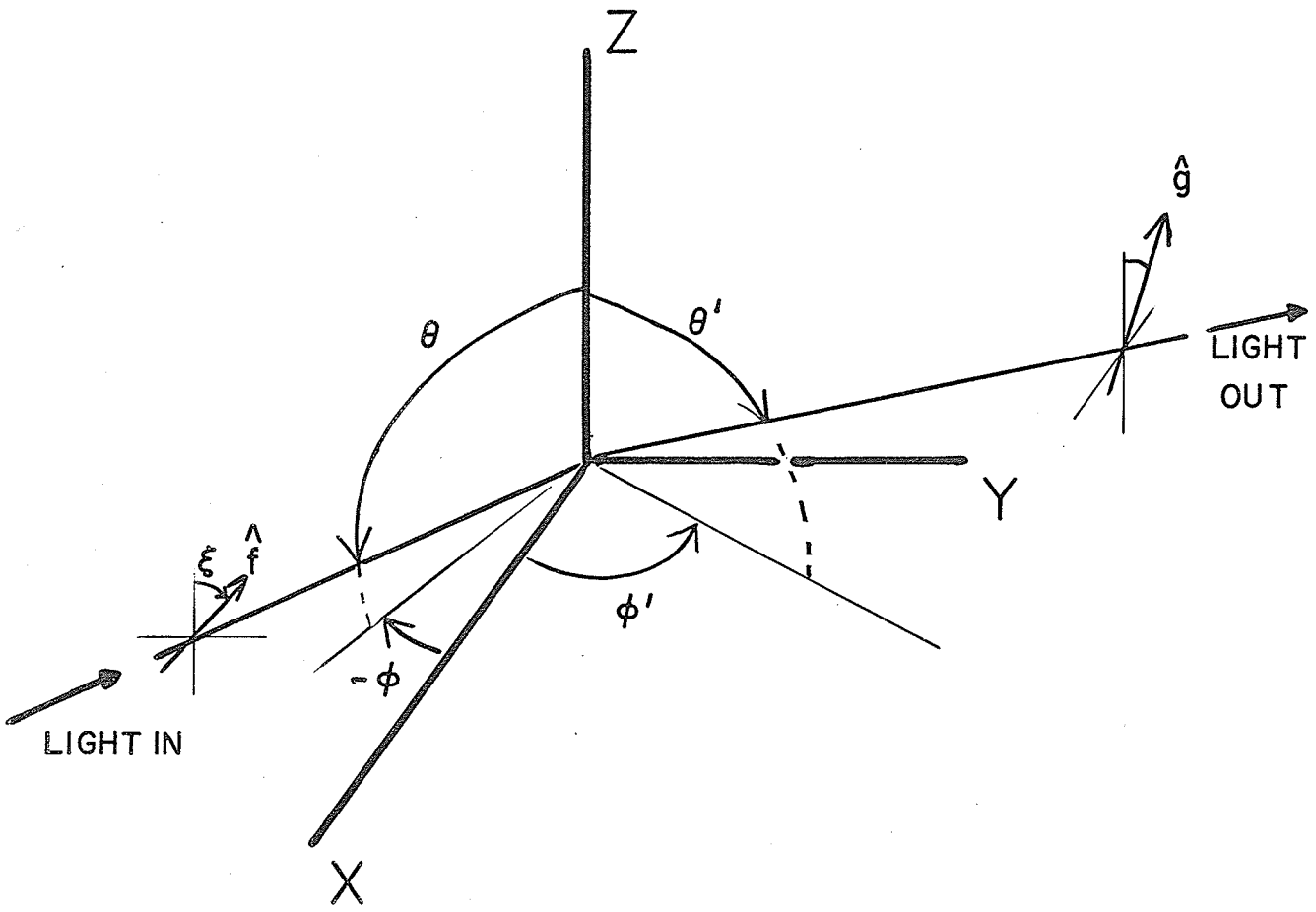
Z
$\hat{g}$
θ
θ'
LIGHT
OUT
Y
$\hat{f}$
ξ
ϕ'
$-\phi$
LIGHT IN
X

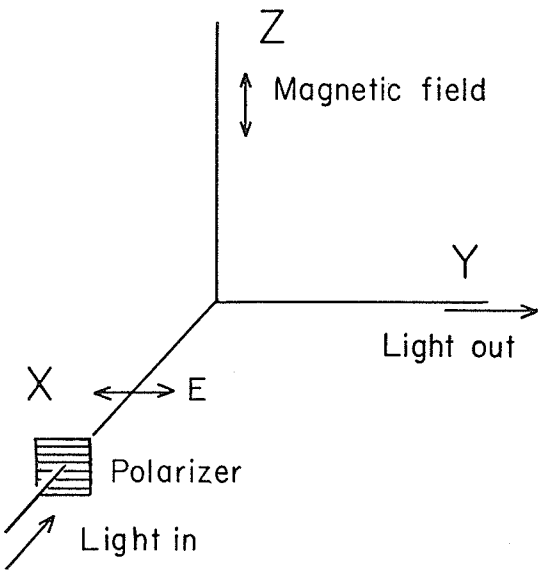
Z
Magnetic field
Y
Light out
X
E
Polarizer
Light in

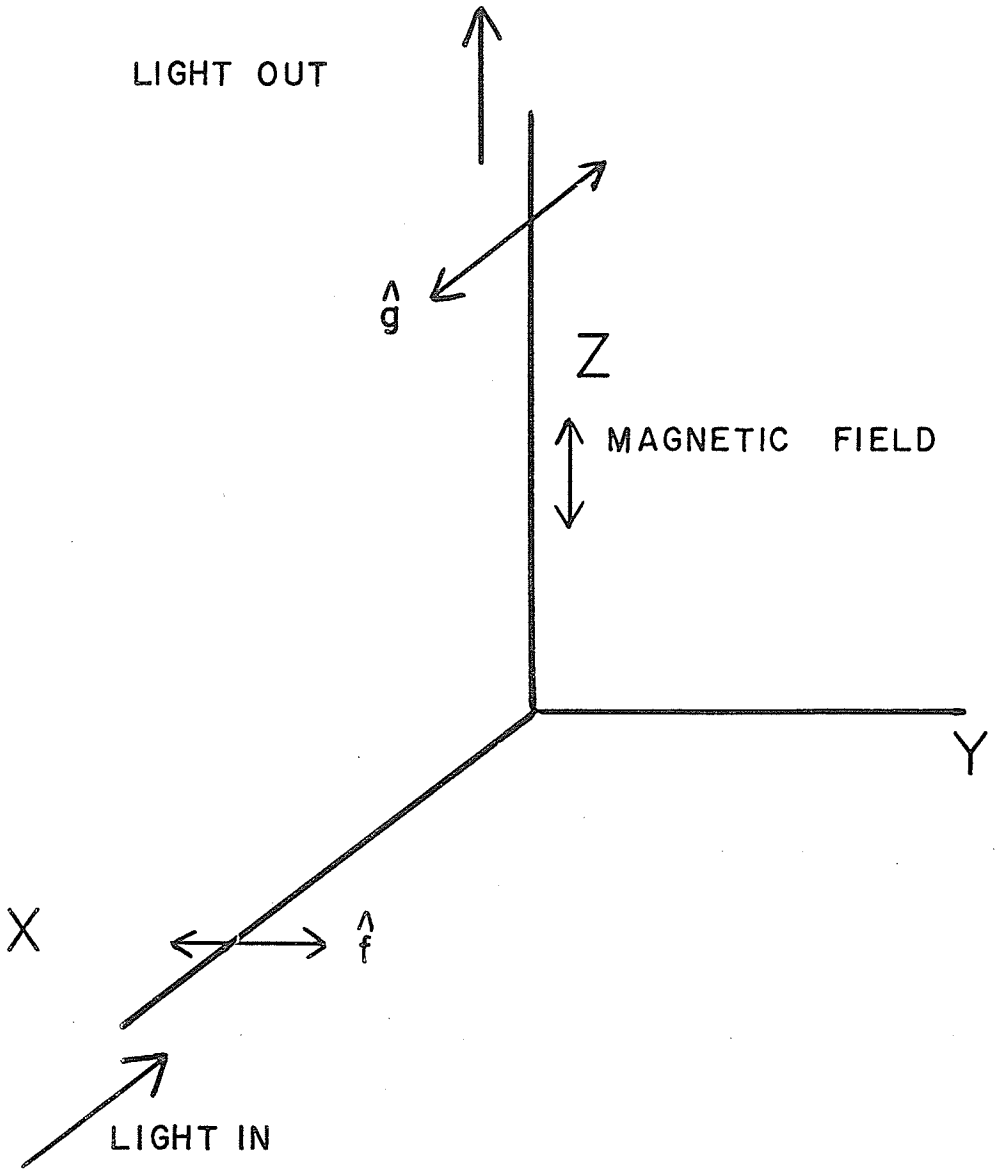
LIGHT OUT
ĝ
Z
MAGNETIC FIELD
Y
X
f̂
LIGHT IN

The source atom decays from the excited state $|\mu>$ to the ground state $|m>$ and emits a photon of frequency ω where $\omega = (E_\mu - E_m)/\hbar + \delta\omega$ and $\delta\omega$ accounts for the Doppler motion of the atom and possibly for other effects such as pressure broadening. The electric field of the light can be represented by

$$\underline{E} = \frac{E_o}{2} \hat{f} \exp(-i\omega t - \gamma t/2)$$

where $\hat{f}$ is the polarization vector of the field, γ is the reciprocal lifetime of the excited level of the source atom, and $E_o/2$ is the amplitude of the field.

At time $t = 0$ this radiation from the source atom is incident on the sample atom. For times $t>0$ the wave function of the sample atom is then a superposition of states, $|\Psi> = \sum_\mu a_\mu(t)|\mu> + b_m(t)|m>$, and in a first order calculation (i.e. the electric dipole or long wavelength approximation) $b_m(t)$ is unity at all times and the a's are given by:

$$a_\mu(t) = \frac{eE_o}{2ih} \cdot <\mu|\hat{f}\cdot\underline{r}|m> \exp(-\frac{\Gamma}{2} - i\omega_\mu)t) \frac{\exp(i(\omega_\mu-\omega)t-\lambda t)-1}{i(\omega_\mu-\omega)-\lambda}$$

In this expression Γ is the reciprocal lifetime of the excited state μ of the sample atom, and $\lambda = \frac{\gamma}{2} - \frac{\Gamma}{2}$. The energy of the stimulated transition of $E_\mu - E_m = \hbar\omega_\mu$, and $\underline{r}$ is the radius vector of the electron that interacts with the photon (see for example Davydov 1965, p. 296, Heitler 1954, p. 196).

The wave function of the atom is (in principle) now known, and the instantaneous rate of spontaneous emission of a photon of polarization $\hat{g}$, as the sample atom decays to the state $|m'\rangle$ is, in the dipole approximation,

$$R(\hat{f}, \hat{g}, t) \propto | \langle \Psi | \hat{g} . \underline{r} | m' \rangle |^2$$

This expression gives the probability of a single sample atom emitting a photon of polarization $\hat{g}$ after the atom is illuminated with a photon of polarization $\hat{f}$ produced by the decay of a source atom. To obtain the total rate of scattering this expression must be integrated over all times, integrated over the frequency spectrum of the incident photons, and summed over all the initial and final states of the sample atom.

To ensure coherent excitation of the two excited states $|\mu\rangle$ and $|\mu'\rangle$ of the sample atom that are involved in the summation, the frequency spectrum of the exciting light must extend over the range $(-E_m + E_\mu)/\hbar$ to $(-E_m + E_{\mu'})/\hbar$ at least in the neighborhood of the level crossing. Franken (1961) and Dicke and Wittke (1960, p. 336) have discussed the equivalence of excitation of the sample atom by light having a broad frequency spectrum when this broad spectrum is the result of the decay of a single source atom having an infinite γ (the pulse excitation of Breit), or the result of the superposition of many incoherent wave trains each having a width γ but separated in frequency by the Doppler effect to give a resultant wave having a broad frequency spectrum.

The photon incident on the sample atom comes from a lamp containing many atoms that are the same as the sample atom. The light (or more correctly the electric field of the light) given out by the decay of any one of these atoms can be represented by the equation given previously. The effect of the incoherent superposition of the light from many atoms will be to give the light some frequency spectrum centred on the frequency of the transition, $\omega_{\mu} = (E_{\mu} - E_{m})\ h$, and extending about this frequency because of the Doppler broadening and the natural lifetime of the source atoms, and it is a good approximation to assume that white light is incident onto the sample atom.

Even without Doppler broadening, the "white-light" approximation is a good one in the absence of hyperfine structure. The natural width of an energy level, ΔE_n, is related to the lifetime of the level, τ, through the Heisenberg uncertainly relation,

$$\Delta E_n \cdot \tau \simeq \hbar$$

The Zeeman splitting of a level is

$$\Delta E_z = g_J \mu_o H$$

and the Hanle signal has its half maximium at a field

$$H_{1/2} = \hbar/(2g_J\mu_o\tau)$$

and in the wings of the resonance the relation

$$\Delta E_z \simeq \Delta E_n$$

will hold. The natural width of the source energy level is thus sufficient to ensure that the frequency spectrum of the incident light extends over the energy levels of the sample atom for the magnetic fields used in a Hanle experiment. The Doppler width is usually much greater than the natural width. The integration over the frequency spectrum can thus be taken between plus and minus infinity.

When the integrations and summations are carried out one obtains the Breit formula;

$$R \propto \text{const.} \sum_{\mu\mu'mm'} \frac{f_{\mu'm} f_{m\mu} g_{\mu'm'} g_{m'\mu}}{\Gamma + i\omega(\mu\mu')}$$

where $\omega(\mu\mu') = \omega_{\mu} - \omega_{\mu'} = (E_{\mu} - E_{\mu'})/h$ and $f_{m\mu} = \langle m|f.\underline{r}|\mu \rangle$. The proportionality constant will depend on the intensity of the incident light and the density of the scattering atoms. The formula applies only in the limit when both of these are small.

The general features of a level crossing, or Hanle resonance, can be seen by considering the form the Breit formula takes in the simple case of a single ground state, m, and two excited states μ and μ'. The level crossing occurs when $E_{\mu} = E_{\mu'}$, and the summation reduces to just two terms,

$$R \propto \frac{A_{\mu\mu'}}{\Gamma + i\omega(\mu\mu')} + \frac{A^{*}_{\mu\mu'}}{\Gamma + i\omega(\mu'\mu)}$$

where in general $A_{\mu\mu'} = \sum_{mm'} f_{\mu'm} f_{m\mu} g_{\mu'm'} g_{m'\mu}$ and $A^{*}_{\mu\mu'} = A_{\mu'\mu}$

This can be re-written as,

$$R \propto \frac{A_{\mu\mu'} + A^{*}_{\mu\mu'}}{1 + [(E_{\mu} - E_{\mu'})/h]^2} - i\frac{(A_{\mu\mu'} - A^{*}_{\mu\mu'})[(E_{\mu} - E_{\mu'})/h]}{1 + [(E_{\mu} - E_{\mu'})/h]^2}$$

and the form the expression takes will depend on the directions and orientations of the polarization vectors through the dipole matrix elements contained in the $A_{\mu\mu'}$.

If $A_{\mu\mu'}$ is real the second term is zero and the first gives a Lorentzian or inverted Lorentzian shaped signal. If $A_{\mu\mu'}$ is imaginary the first term is zero and the second gives a dispersion shaped signal. In general the signal is some combination of the two.

It is interesting to note that in the important paper of Franken (1961) an error of sign occurs. The only effect of this is to change the sign of the dispersive shaped term. Usually this term is made zero by a suitable choice of geometry so the mistake went unnoticed until Stroke et al (1968) pointed out that the sign of the second term depends on the ordering of the levels μ and μ' Examination of the sign of the dispersive term thus allows the order of the energy levels and hence the sign of the interaction constants to be determined.

A number of authors have given general expressions for the form of the level crossing signal; for example, Stroke et al (1968), Lurio, deZafra and Goshen (1964), Fry and Williams (1969).

For most of the Hanle experiments described in this work the geometry is as shown in Fig. 11 (ii), or in Fig. 11 (i) with $\theta = \theta' = \phi' = 90^{\circ}, \phi' = 0$, and $\xi = 90^{\circ}$. No polarization analyser is used in the output arm. Some experiments were also done with the 90 - 90 - 90° geometry of input, output, and magnetic field directions but with no polarizer on the input arm, and some by observing the light emitted along the Z direction, with a polarizer on the input arm and an analyser in the output arm set to pass light with the electric vector either along the X axis or alternatively along the Y axis.

For the even isotopes of barium the ground state, $6s^2\ {}^1S_0$, has only the single Zeeman state m = 0. The ${}^1P_1$ levels $6snp\ {}^1P_1$ n= 6,7,8, have three Zeeman states m = 1, 0, -1. There

are then nine terms in the summation for R. The Zeeman splitting of the ^1P states is,

$$E_\mu = g_J \mu_o H m_\mu = \nu h m_\mu \quad ,$$

and the expression for R can be written as,

$$R \propto \sum_{\substack{\mu\mu' \\ mm'}} \frac{f_{\mu' m} f_{m\mu} g_{\mu' m'} g_{m'\mu}}{1 + 2\pi\tau\nu(m_\mu - m_{\mu'})}$$

where $\tau = 1/\Gamma$.

The nine terms are then,

$$R \propto f_{10} f_{01} g_{10} g_{01} + f_{00} f_{00} g_{00} g_{00} + f_{-10} f_{0-1} g_{-10} g_{0-1}$$

$$+ \frac{f_{10} f_{00} g_{00} g_{01}}{1 - 2\pi i\tau\nu} + \frac{f_{10} f_{0-1} g_{-10} g_{10}}{1 - 4\pi i\tau\nu} + \frac{f_{00} f_{01} g_{10} g_{00}}{1 + 2\pi i\tau\nu}$$

$$+ \frac{f_{00} f_{0-1} g_{-10} g_{00}}{1 - 2\pi i\tau\nu} + \frac{f_{-10} f_{01} g_{10} g_{0-1}}{1 + 4\pi i\tau\nu} + \frac{f_{-10} f_{00} g_{00} g_{0-1}}{1 + 2\pi i\tau\nu} .$$

The required matrix elements are given by Condon and Shortley (1963 p63) and are,

$$f_{0\pm1} = \mp \frac{1}{\sqrt{2}} \hat{f}.[\hat{i} \pm i\hat{j}] \langle||r||\rangle = f^*_{\pm10}$$

$$f_{00} = \hat{f}.\hat{k} \langle||r||\rangle$$

where $\hat{i}\ \hat{j}\ \hat{k}$ refer to the unit triad, $\langle||r||\rangle$ is the reduced matrix element, and $\hat{f}$ and $\hat{g}$ are the input and output polarization directions respectively. For the geometry used $\hat{f} = \hat{j}$ and since no polarizer is used in the output arm the contributions of the two perpendicular components $\hat{g} = \hat{k}$ and $\hat{i}$, must be added. The reduced matrix elements can be included in the constant.

The terms of the sum can be split into three groups characterized by the change in the magnetic quantum number, $\Delta m = 0, 1,$ and 2. Using the angles shown in Fig. 11 (i) and the polarization directions described above these three groups are,

$\Delta m = 0 \qquad 2 - \sin^2\theta'$

$\Delta m = 1 \qquad 0$

$\Delta m = 2 \qquad \{\sin^2\theta' \cos 2(\phi-\phi')\} / \{1 + x^2\}$

$$+ \{x \sin^2\theta' \sin 2(\phi-\phi')\} / \{1 + x^2\}$$

where $x = 2g_J \mu_o H / \hbar$.

When the incident light is plane polarized with the electric vector in the X-Y plane (as shown in Fig. 11 (ii)) the Hanle resonance is due to the $\Delta m = 2$ terms only. This result has a simple semi-classical explanation.

The plane polarized light can be considered as the superposition of two contra-rotating circularly polarized beams. One of these carries a component of angular momentum +1 the other -1, and there is a definite phase relation between them. The $m_J = +1$ and $m_J = -1$ Zeeman states are excited coherently and when these two states are separated by less than their natural widths interference effects are possible.

For the 90-90-90 geometry used in our experiments the expression for the rate of absorbtion and subsequent emission of the polarized resonance radiation is the sum of the three

terms for $\Delta m = 0$, 1, and 2:

$$R \propto \text{const.}\left(1 - \frac{1}{1 + (2\tau g_J \mu_o H/\tau)^2} \right)$$

The constant of proportionality depends on the number of incident photons, the number of scattering atoms and the oscillator strength of the transition. In practice, the signal will also depend on the solid angles subtended by the detector and by the exciting lamp; Budick (1967) has given estimates of the signal strength for double resonance and level crossing experiments and he suggests that in the level crossing case the resonant signal may be only 15% of the non-resonant one.

The expression derived above is valid only when the probability of absorbtion and subsequent emission is small.

If no polarizer is used on either the input or output directions the effect is to double the constant or field independent contribution (for the 90^o-90^o-90^o geometry). Classically the explanation is simple; a dipole excited along the Z direction is not affected by a magnetic field in the Z direction. The intensity observed along the Y axis is then the sum of this constant contribution plus that due to the dipole in the X-Y plane.

For the geometries used in all experiments whose results are used the shape of the Hanle resonance is an inverted Lorentzian; for these resonances if the full width at half maximium of the curve is ΔH, then the lifetime of the level

is given by,

$$1/\tau = \mu_o \, g_J \, \Delta H/h \ ,$$

and to obtain the lifetime the g_J value of the level must be known.

DEPARTURES FROM THE IDEAL CASE: THE EFFECTS OF GEOMETRY, ODD ISOTOPES, AND COHERENCE NARROWING.

In obtaining these results it has been assumed that the incident and scattered angles are exactly 90°. In fact light is collected over small solid angles about these directions and what is observed is not the expression given but its average over small solid angles centered on the ideal 90-90-90 geometry. Fry and Williams (1969) show that if the angles range over the small amounts (refer to Fig. 11 (i)),

$$\theta \quad 90^{\circ} \pm \gamma \qquad\qquad \theta' \quad 90^{\circ} \pm \delta$$

$$\phi \quad \pm \alpha \qquad\qquad \phi' \quad 90^{\circ} \pm \beta$$

$$R \propto \frac{2\alpha}{\sin 2\alpha} \cdot \frac{2\beta}{\sin 2\beta} \cdot \frac{3+\sin^2\delta}{3-\sin^2\delta} - \frac{1}{1+(2g_J\mu_o H/h)^2}$$

In the limit $\alpha, \beta, \gamma, \delta, \rightarrow 0$ this tends to the previous result. For finite angles the first term in the above expression is greater than one; at zero field the signal is thus not zero and a field independant background has been added to the signal. The shape of the resonance is not affected. For the experiments described, the lenses used have a diameter of 2.5" and a focal

length of 10"; they therefore collect light over a cone of half angle 0.125 radians. This adds 3% to the background. Departure of the scattering angle from 90° can also introduce a dispersive component into the signal. As an approximation the expression for R can be written

$$R \propto \{ \; 1 - \frac{A}{1 + x^2} + \frac{Bx}{1 + x^2} \; \}$$

If the departure from the ideal geometry is small the magnitude of A is close to one and that of B small; if $\phi - \phi'$ (Fig. 11 (i)) departs from 90° by 1°, $A \approx 0.97$ and $B \approx 0.03$.

Of the seven stable isotopes of barium the two odd ones, 135 and 137, occur with abundances of 6.6 and 11.3% respectively for a total of 17.9% odd isotopes; most (71.7 out of 82.1%) of the remainder in the natural mixture is Ba^{138}. Both odd isotopes have spin I = 3/2 and small departures from pure LS coupling which lead to a small magnetic hyperfine structure in the 6snp $^1P_1$ levels and this might be expected to affect the shape of the Hanle resonance. The nuclear angular momentum of these isotopes alters the angular momentum quantum numbers for the atomic scattering system and hence affects the angular distribution of the scattered resonace radiation. The level crossing signal of the odd isotopes is then different from that of the even isotopes, (for which the nuclear angular momentum is zero) even though the lifetime of the level is unchanged.

The overall splitting of the $6s6p\,^1P_1$ level of Ba^{137} is about 500 MHz (Lurio 1964) while the Doppler width at 0 °C is about 600 MHz. A theoretical prediction of the shape of the Hanle signal of the odd isotopes is difficult; see for example, Lurio and Novick (1964) where the case of cadmium is discussed. The level crossings at non-zero field occur at about 150G for the barium $6s6p\,^1P_1$ level (Lurio 1964) and so are well beyond the wings of the Hanle resonance. However, in view of the smallness of the hyperfine structure in relation to the Doppler effect and the quite large concentrations of the odd isotopes one might expect that the effect of the odd isotopes is important. To check this, Lurio (1964a) obtained a sample enriched to 98% in Ba^{138} and found no difference between the width of the Hanle resonance given by this sample from that given by the natural barium. The precision of his experiments was comparable to those described here, that is about 2%.

The hyperfine structure of the $^3P_1$ level is much larger than that of the $^1P_1$ level and zuPutlitz (1963) has discussed the magnetic "tuning" of the frequency of transitions between the Zeeman states of the even isotopes in a source to ensure maximium absorption by the odd isotopes in a beam for this case.

The width of a Hanle resonance is not independent of the density of the scattering atoms. In a Hanle experiment, an incoming resonance photon excites a sample atom that subsequently

decays with the emission of another photon. This photon may escape from the scattering region or it may be absorbed by a second sample atom. If all the sample atoms are in the same magnetic field the time variation of the wave functions representing the excited states will be the same and phase information - such as the orientation of the atom in the excited state - can then be transfered from one atom to another by the photons. This multiple scattering of the radiation leads to an apparent longer lifetime of the excited state and consequently to a narrowing of the Hanle resonance called coherence narrowing. The extent to which the radiation is multiply scattered before escaping will depend on the density of the scattering atoms, and in the extreme case the radiation can be completely trapped. At very low densities all the Zeeman states of an excited level decay with the natural lifetime of that level and under these conditions the width of the Hanle resonance is inversely proportional to the lifetime. At higher densities the Zeeman states can relax to each other by radiation trapping (and collision broadening), and the observed width is no longer inversely proportional to the lifetime. These effects have not entered the theory that has been discussed up to this point because the theory has been developed in terms of a single atom rather than an ensemble of atoms for which the density matrix formalism is most frequently used.

In general, an optically excited atomic state having total angular momentum J has associated with it 2J + 1 multipole

moments. For the cases of interest here the ground state has $J = 0$ while the excited state has $J = 1$, and the three quantities or moments are the population, the orientation (or magnetic moment of the excited state), and the alignment (or atomic polarization with zero magnetic moment) of the excited state.

When the interactions between the atoms making up an ensemble are considered, each of the $2J + 1$ (ensemble averaged) multipole moments no longer decays with the natural lifetime of the state. The (ensemble averaged) multipole moments of the ensemble are proportional to the corresponding multipole components of the density matrix representing the system and the lifetimes that can be observed in a Hanle experiment can be related to the different relaxation times of the multipole components of the density matrix, (Happer and Saloman, 1967; Saloman and Happer 1966).

When only electric dipole transitions are considered two lifetimes can be observed; these are called the orientation lifetime τ_1 and the allignment lifetime τ_2. Using plane polarized light (as was done in the experiments described) only the alignment lifetime τ_2 can be observed but if circularly polarized light is used both lifetimes can be observed. Both lifetimes tend to the natural lifetime of the excited state as the density becomes small and in any experiment the geometry, orientation, and type of polarizers used will determine which of the two is observed.

Coherence narrowing in a Hanle experiment was first observed and explained by Barrat (1957, 1959) who showed that the lifetime obtained by extrapolating to zero density agreed with the results obtained from double resonance and level crossing experiments. Barrat used the density matrix formalism in developing the theory of coherence narrowing, as did d'Yakanov and Perel' (1965) who used a more realistic Boltzman velocity distribution for the scattering atoms than the constant velocity assumed by Barrat. Saloman and Happer (1966) extended the theory to allow for branching from the excited state, and Piper and Sandle (1970) have taken account of the variation in scattering atom density in the scattering region. The validity of the theoretical results has been demonstrated by the authors mentioned. Coherence narrowing in closely related to radiation trapping and Holstein (1947, 1951) has given a full treatment of this.

The theories of Barrat, or the more refined theory of d'Yakanov and Perel', show that the measured width of the Hanle resonance, Γ_2, is related to the natural width of the level, Γ, by

$$\frac{\Gamma}{\Gamma_2} = 1 - A_2 x$$

where A_2 is a function of the angular momentum quantum numbers of the excited and ground levels, and x is the probability for multiple scattering of a photon in the scattering region.

If j_0 is the angular momentum of the ground state and j_1 of the excited state then

$$A_2 = \frac{7}{100} \cdot \frac{[\,3Y(Y-1) - 8j_1(j_1+1)\,]^2}{(2j_1-1)2j_1(2j_1+2)(2j_1+3)}$$

where $Y = (j_1 - j_0)(j_0 + j_1 + 1) + 2$

and x depends on the characteristic dimension of the scattering region, L, and the mean free path of a photon at the centre of the line,

$$x = 1 - (1/\sqrt{\pi}) \int_{-\infty}^{\infty} \exp(-t^2).\exp\left(-\frac{L}{l_0} e^{-t^2}\right) dt$$

the integral is tabulated in Mitchell and Zemansky (1934). The parameter l_0 depends on the thermal velocity, v_0 and density, n_0, of the scattering atoms and on the wavelength of the photon,

$$l_0 = \frac{2j_0 + 1}{2j_1 + 1} \quad \frac{8\pi^{3/2} v_0}{n_0 \lambda^3 \Gamma}$$

In the linit $L >> l_0$, the high density limit, d'Yakanov and Perel' (1965) show that the integral expression for x can be approximated by,

$$x = 1 - (l_0/L).1/\sqrt{[\pi \ln(L/l_0)]} \ .$$

RELATIONSHIP OF LIFETIME OF A LEVEL TO THE OSCILLATOR STRENGTHS OF TRANSITIONS FROM THE LEVEL.

The radiative lifetime, or mean life, of an excited state can be expressed in terms of the electric dipole transition matrix elements of transitions to lower energy levels. If the wavelengths of the transition $n \rightarrow m$ is λ_{nm}, the lifetime of the level n is given by (Heitler 1954, Condon and Shortley 1963, Davydov 1965)

$$1/\tau = \sum_m \frac{64}{3} \frac{\pi^4 e^2}{\lambda_{nm}^3} \frac{1}{h} \left| \langle n | \underline{r} | m \rangle \right|^2 ,$$

where $\underline{r}$ is the position vector of the electron involved in the transition and the sum extends over all lower states m.

It is usual to express the lifetime in terms of the Einstein coefficients for spontaneous emission A_{nm}, and the absorption oscillator strengths, or f-values, f_{mn};

$$1/\tau = \sum_m A_{nm}$$

$$A_{nm} = \frac{8\pi^2 e^2}{mc} \frac{1}{\lambda_{nm}^2} \frac{g_n}{g_m} f_{nm} ,$$

$$f_{mn} = \frac{8\pi^2}{3} \frac{g_n}{g_m} \frac{mc}{h\lambda_{nm}} \; | < n | \underline{r} | m > |^2$$

g_n and g_m are the statistical weights of the levels n and m respectively. The absorption oscillator strength of the $n \rightarrow m$ transition f_{mn} is a measure of the ability of the atom to absorb radiation as compared with a classical oscillating electron.

Numerically one has

$$A_{nm} = \frac{1}{1.499} \frac{g_m}{g_n} \frac{f_{mn}}{\lambda_{mn}^2}$$

with the wavelength in cm.

If either the f-values of the transitions from a level, or their ratios, called the branching ratio, are known the lifetime as determined from the Hanle experiment can be compared with the lifetime obtained from the sum of the A coefficients. Alternatly if only the branching ratio is known the lifetime obtained from a Hanle experiment can be used to determine the absolute f-values.

Crossley (1969) has reviewed methods of calculating f-values, while Foster (1964) and Wiese (1968) have reviewed experimental methods.

In calculating f-values of transitions in many

electron elements such as barium, configuration interaction, intermediate coupling, and the lack of satisfactory wave functions seriously limit the accuracy and reliability of the results.

Experimental methods of obtaining f-values can be split into two categories; those that depend on a knowledge of the vapour density, and those that do not.

Typical of the former is the hook method of Rozhdestvenskii which has been used by Penkin and co-workers (Ostrovskii and Penkin 1960) to measure the f-values of many lines in the barium spectrum. In this method the anomalous dispersion of the vapour of the element being studied is measured.

Relative f-values given by this method, and by absorption methods, should be accurate, but to obtain absolute f-values the vapour density must be known. Measurements of vapour density are difficult, often unreliable, and lead to uncertainties of at least 10% and frequently to much larger systematic errors (see for example Foster 1964).

The Hanle effect is a good example of a method that can be density independent. Rather than determining f-values directly the lifetime of a level is determined and in conjunction with the relative values given by other methods absolute f-values are obtained.

CHAPTER IV RESULTS

INTRODUCTION

Hanle resonances were observed in the 6s6p, 6s7p, and 6p5d, $^1p_1$ configurations using the transitions from these levels to the $6s^{21}S_0$ ground state at 5535, 3071.58, and 3501 Å respectively.

The Hanle resonance of the 6s8p $^1P_1$ level via the transition 6s8p $^1P_1 \rightarrow$ $6s^2$ $^1S_0$ 2785 Å, was searched for but not observed.

6s6p $^1P_1$

The Hanle effect of the $6s6p^1P_1$ level was observed in the resonance line $6s^2$ ^1So - $6s6p^1P_1$, 5535 Å and a plot of a typical Hanle resonace is shown in Fig. 12; this is the graph that the computer plots on the line printer. The data was obtained using the first of the two experimental set-ups described previously. In Table III are given the experimental results. These are the best results chosen for the following criteria; (a) the slope of the base-line of the fitted curve is small, indicating that the beam density remained constant during the run. A separate check was made of the lamp intensity before and after each run. This was done by measuring the number of counts in a given period (1 or 10 seconds) with the beam cut off by the beam flag, ie. the number of photons reflected from the inside

Fig.12 Hanle effect of $6s6p\,^1P_1$.

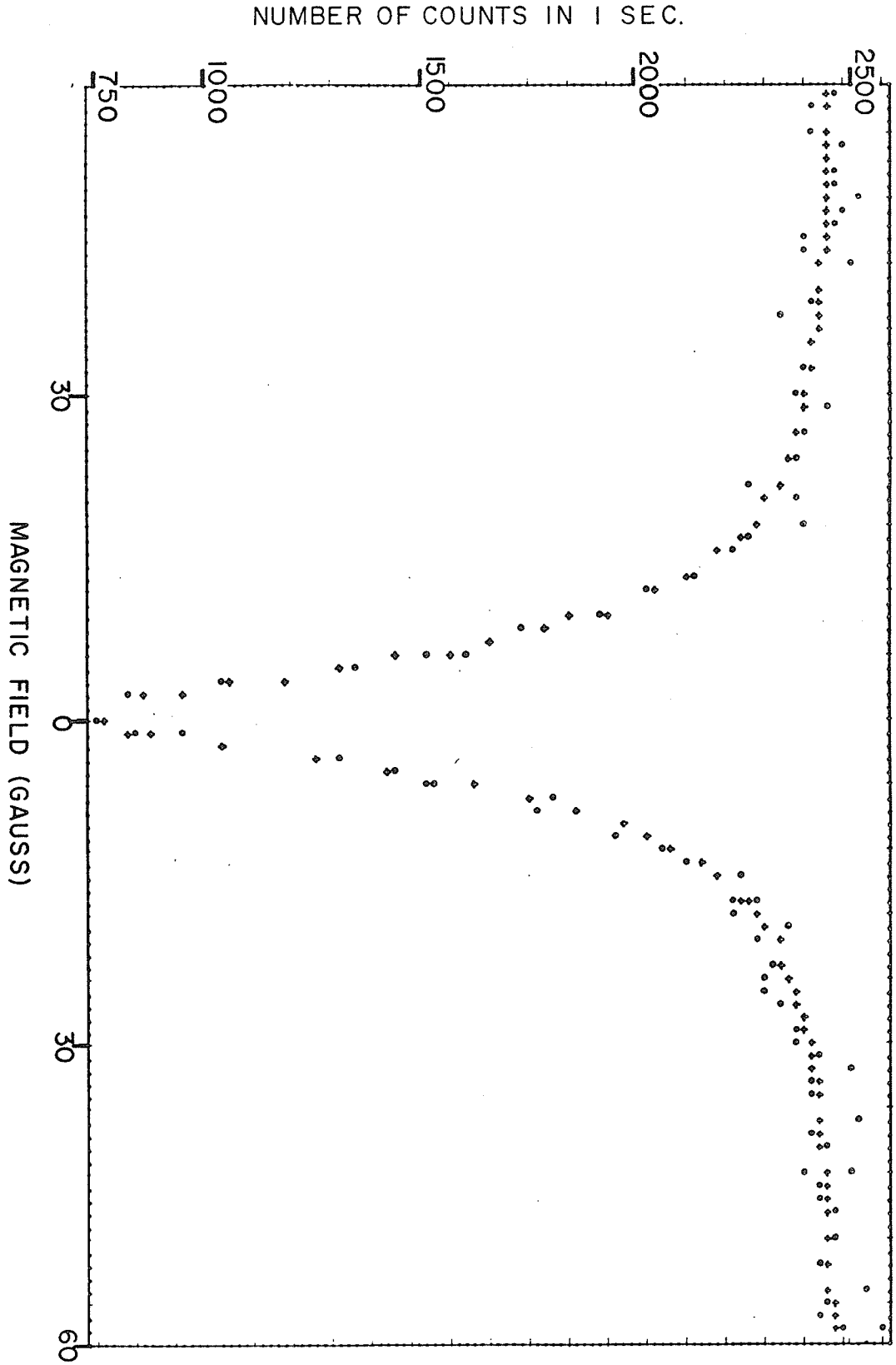
NUMBER OF COUNTS IN 1 SEC.
750
1000
1500
2000
2500
30
0
30
60
MAGNETIC FIELD (GAUSS)

of the vacuum chamber was measured. Only those runs with a very small change in lamp intensity (less than 1%) and a change in signal size due to change in beam density of less than 5% are given in Table III.

(b) The value of the error parameter given by the program indicated that the points could be properly fitted to a Lorentzian, and that the error in the full width at half height was reasonable. The goodness-of-fit is determined by the value of $F = \Sigma ((Y_{calc} - Y_{exp})^2/Y_{exp})$ where the sum extends over the N data points and the fit is considered good if F is in the range N to about 1.5N. At very low beam densities statistics are poor and sometimes the fit is poor. At the highest densities a discharge sometimes developed at the mouth of the furnace; the resonance radiation from this discharge gave the expected signal shape. This discharge was usually detected when the lamp intensity was being checked. In addition some curves taken at high densities showed departures from the ideal symmetric shape due to an effective change in the scattering angle and the resulting addition of some dispersion shaped signal to the output; such curves were not used.

Coherence narrowing of the Hanle resonance was observed. The density of the scattering atoms is not known but the normalization constant, I_0, in the Hanle expression is proportional to both the beam density and the lamp intensity (Franken 1961).

TABLE III

Hanle Effect of $6s6p\,^1P_1$ 5535 A

Run Number	Full Width $\frac{1}{2}$ Height	Density Parameter
78	14.17	2.994
79	13.81	4.861
81	13.38	6.011
82	13.15	6.103
83	13.55	6.560
84	13.12	13.48
85	12.38	15.579
86	11.96	14.299
87	12.93	28.477
88	12.45	31.491
89	10.66	61.315
90	10.50	65.989
91	13.04	43.024
92	10.27	70.658
96	13.37	.558
97	13.28	.522
106	13.31	.384
113	10.60	29.38
125	14.65	1.606
130	13.37	11.97
131	12.78	17.11
132	13.41	18.60
133	13.87	18.93
134	11.58	20.16
137	13.01	13.07
138	11.26	38.92
139	10.98	36.65
140	10.76	36.93
143	12.96	1.12
144	14.39	1.78
145	14.41	1.84
146	13.19	8.13

This constant, normalized to constant input light intensity is used as a density parameter and is given in the table of results. The same procedure has been used by Landmann (1968) in Hanle experiments in Argon where some metastable levels were used as the initial levels.

To allow for the coherence narrowing the measured widths, Γ_2, of the Hanle resonances have to be fitted to the relation given earlier,

$$\Gamma/\Gamma_2 = 1 - A_2 x \ .$$

For the transition 6s6p $^1P_1 \rightarrow 6s^2\ ^1S_0$, $A_2 = 0.7$. Because the density, n_0, of the scattering atoms is not known, x cannot be calculated. However, the observed narrowing is small and changes only slowly as I_0 changes over several orders of magnitude. In addition some indication of the size of x and of its dependence on the beam density, n_0, can be obtained from the known parameters of the system. From preliminary results the lifetime $\tau = 1/\Gamma$ is about 8.10^{-9} seconds and by assuming that the thermal velocity of the scattering atoms is equivalent to 500°C, (approximately the temperature of the furnace) the mean free path is $l_0 = 1.537.10^{10}/n_0$ cm, where the density is in atoms cm^{-3}. The beam has a diameter of 1 or 2 cm at the scattering region, so the so-called characteristic dimension, L, can be put equal to 2cm. The ratio l_0/L is then small (of the order of 1 if $n_0 = 10^{10}$ atoms cm^{-3}) and it can be assumed that the variation of x with density, i.e. with l_0/L, will be linear. The experimental values of the width of the resonance

were fitted, using least squares, to the density parameter I_0. Figure 13 is a plot of the fit showing the variance expected in any point. The intercept with the zero axis is 13.58 ± 0.21G. The error is obtained by combining the standard deviation of the intercept with the axis and the uncertainty in the calibration and measurement of the magnetic field. Then, to take account of possible unknown systematic errors and the approximation involved in the straight line extrapolation, the error is multiplied by 5 to give a total error of 1.6%.

At the highest density of the scattering atoms shown in the figure, the ratio of the measured width to the zero density width is 10.27:13.58 or 0.7:1. If this ratio is substituted into the coherence narrowing formula, using the estimates of the parameters given earlier, the density of the scattering atoms is about 5.10^9 atoms cm^{-3}. It is at about this density that the shape of the coherence narrowing curve begins to depart significantly from a straight line. If the last three points shown in the graph are omitted from the least squares calculation the zero intercept is changed only slightly to 13.52 $\pm$ 0.21 (c.f. 13.58) while both the calculated density, and the value of the density parameter, are reduced by about one half at the highest density then used. At this density the approximations involved in making the straight line extrapolation and in using the amplitude of the Lorentz peak as an index of beam density are valid. At the lowest beam densities used the count rates are low and statistics are poor resulting in a rather large scatter

Fig.13 Experimental dependence of full width at half height on scattering atom density.

the vertical scale is Gauss,the horizontal scale is index of beam density in arbitrary units.

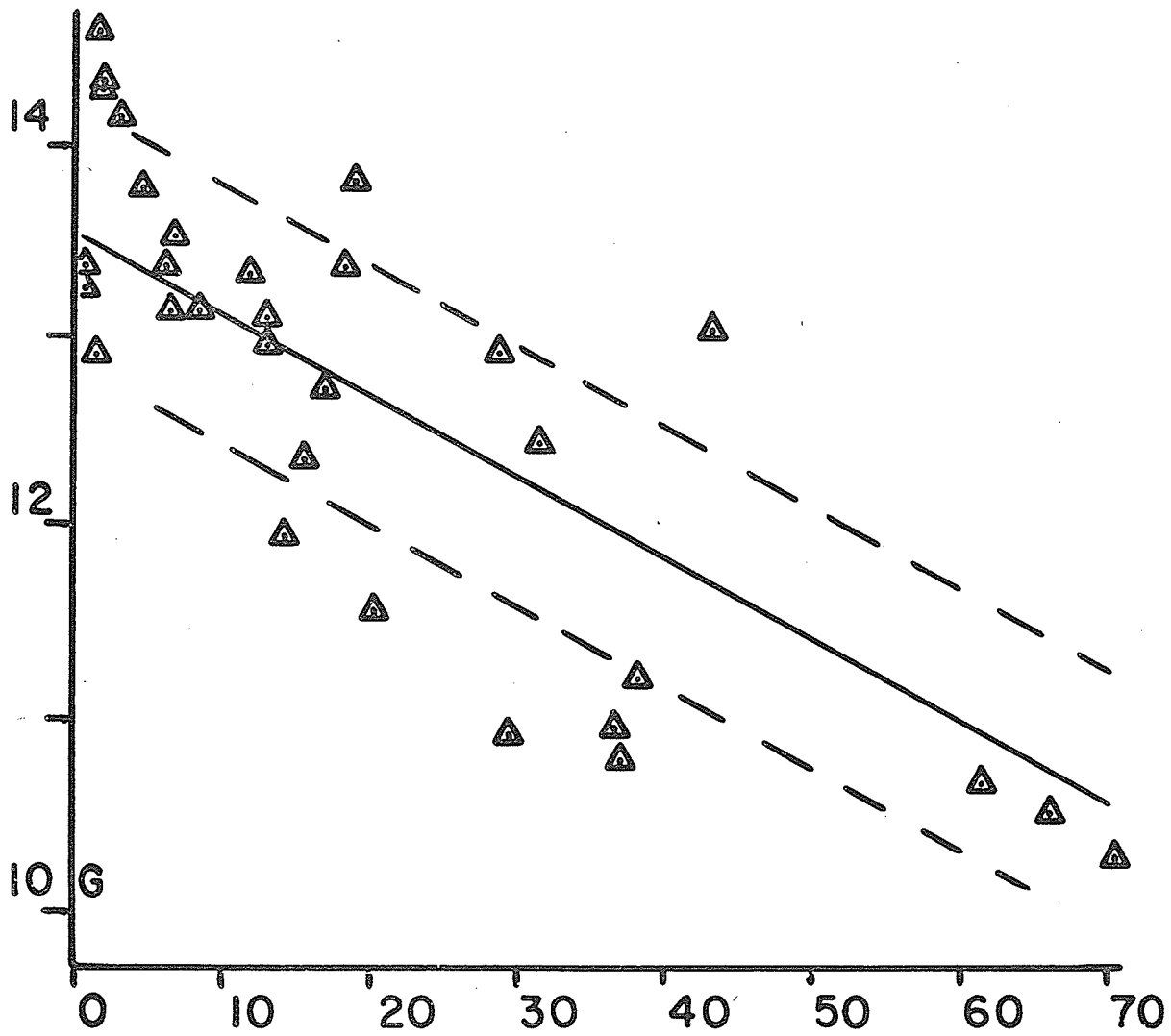
14
12
10
G
0
10
20
30
40
50
60
70

of the experimental points but these points are important because of the logarithmic dependence of the width on the density. For these reasons a least squares fit to a straight line over a range of densities gives a more reliable result.

The two values for the intercept with the zero axis agree within the estimated errors and using the smaller value, obtained without the high-density points, and the g_J value given by Swagel and Lurio (1968) the lifetime is;

$$\tau(6s6p\,^1P_1) = 8.37 \pm 0.14 \quad 10^{-9} \text{ sec.}$$

This result, and other quantities relating to this level, are collected in Table IV.

From our value of the lifetime, which is in excellent agreement with previous results, the oscillator strength of the 5535 Å transition can be determined.

This oscillator strength is important because the relative oscillator strengths, or f values, of the series $6s^2\ ^1So - 6s\,np\ ^1P_1$ for n = 6 up to n = 18 are known from the work of Penkin and Shabanova (1962) and once the absolute oscillator strength of the principle line of the series is known the others can be obtained. In addition, almost all the most accurately known absolute oscillator strengths in

TABLE IV

Experimental and Theoretical Quantities Relating to The $6s6p\,^1P_1$ State of Barium

Life time - Experimental		
Bucha and Schussler	(1961)	$10.4\pm0.5 \times 10^{-9}$ sec
Hulpke Paul and Paul	(1964)	8.36 ± 0.25
Lurio	(1964)	8.37 ± 0.20
This Work		8.37 ± 0.14
Oscillator Strengths - Experimental		
f(5535)		
Wessel (1949,1951)		1.8 ± 0.25
Ostrovskii Penkin and Shabanova (1958)		1.7 ± 0.2
Penkin and Shabanova (1962)		1.40 ± 0.05
Miles and Wiese (1969)		1.59
Lurio (1964)		1.55 ± 0.06
f(15000)		
Hulpke Paul and Paul (1964)		0.10 ± 0.02
Oscillator Strengths - Theoretical		
f(5535)		
Bates and Damgard (see Lurio 1964)		1.92
Freidrich and Trefftz (1969)		1.88
f(15000)		
Freidrich and Trefftz (1969)		$0.02\sim0.51$
g_j Value - Experimental		
Swagel and Lurio (1968)		1.0039 (8)

the barium spectrum are obtained from f(5535) in the same manner -- as is discussed by Miles and Wiese (1969) in their critical compilation of the barium oscillator strengths. Miles and Wiese suggest that the data of Penkin and Shabanova (1962) and of Ostrovskii and Penkin (1960) is the most reliable. These results were obtained with the hook method.

To obtain the oscillator strength from our value of the lifetime, the small contribution of the $6s6p\,^1P_1 - 6s5d\,^1D_2$ 15000 Å transition to the (two term) sum,

$$1/\tau = \sum_n A_{nm} = \frac{1}{1.499} \sum_n \frac{g_n f_{nm}}{g_m \lambda_{nm}^2}$$

must be considered. Hulpke, Paul, and Paul (1964) estimate f(15 000) at 0.10 ± 0.02 from Stark effect measurements by Paul and the method of f-sums. They estimate the maximum possible value of f(15 000) at 0.48 ± 0.34 from the results of a calculation using the Bates and Damgard approximation.

Lurio (1964) has given f(15 000) = 0.17 ± 0.06, and, using this value, the oscillator strength of the 5535 Å line is f(5535) = 1.57 ± 0.6, where the longer wavelength line contributes about 7% to the sum of the A values. Using Pauls value of 0.10 we obtain f(5535) = 1.60 ± 0.3, and the contribution of the longer line is about 4%, while their limiting value, f(15 000) = 0.48, yields f(5535) = 1.44. Miles and Wiese give f(5535) = 1.59 and estimate the errors as, "within

10%." They obtained this value from the lifetime results of Lurio and of Hulpke et al after allowing for the effect of the long wavelength transition.

Since the lifetime of the $6s6p\,^1P_1$ level obtained in this work is essentially the same as that obtained by Lurio and by Hulpke, Paul and Paul, the agreement between the oscillator strength results is as expected and it seems reasonable to adopt Miles and Wiese's value as it would appear that they have chosen to adopt some average value of f(15 000) in obtaining f(5535) = 1.59.

$6s7p\,^1P_1$

The Hanle resonance of the $6s7p\,^1P_1$ level was obtained using the transition $6s^2\ ^1So$ - $6s7p\,^1P_1$, 3072 Å and the same geometry as was used for the 6s6p level. The data was collected using the multichannel analyser as a signal averager as described previously. A plot of a typical curve and the fitted Lorentzian is shown in Fig. 14 and the results are given in Table V. The oscillator strength of the 3072 Å transition is small and no evidence of coherence narrowing was observed.

Runs were made with different beam densities, different lamp intensities and different sweep periods of the scanning magnetic field. No systematic trends were observed.

Fig.14 Hanle effect of $6s7p\ ^1P_1$.

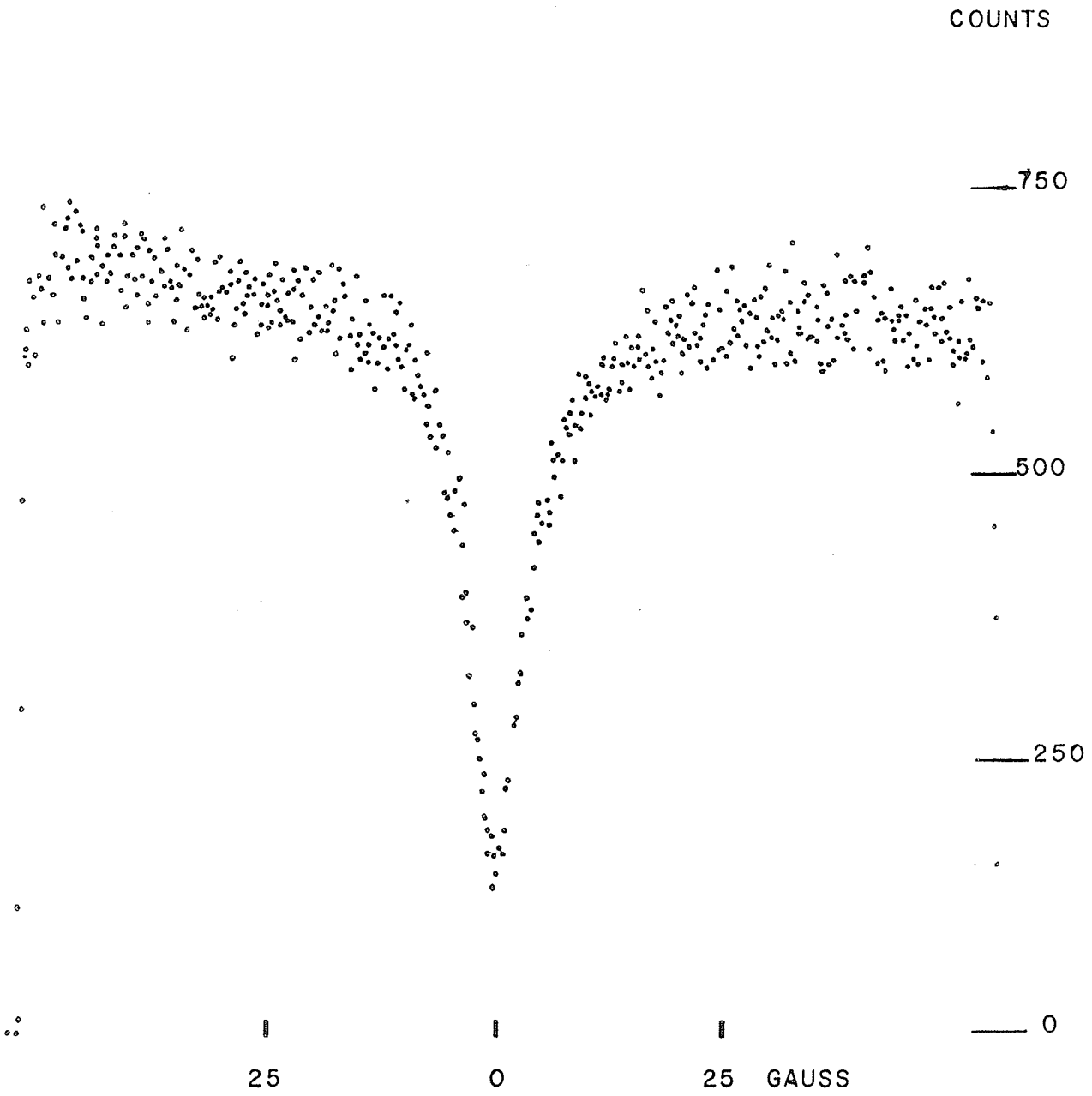

3501 1-7-1-91

TABLE V

Hanle Effect of $6s7p\,^1P_1$, 3072 Å

Full Width $\frac{1}{2}$ Height (Channels)
36.55
29.33
32.41
30.66
35.12
35.30
33.88
34.19
39.05
36.66
30.77
28.31
30.22
Mean 33.22 ± 1.06
In Gauss 8.59 ± 0.25

The mean of fourteen determinations of the full width at half height of the Hanle resonance is 8.59 ± 0.25G from which

$$g_J\tau = 13.2 \pm 0.4.10^{-9} \text{ sec.}$$

The g_J value of this level has been measured by Ma et al (1970) as

$$g_J(6s7p\,^1P_1) = 1.003(2).$$

This group also found $\tau = 13.4(6) . 10^{-9}$ sec. in good agreement with our result. The results are collected in Table VI.

To obtain the oscillator strength of the transition from the $6s7p\,^1P_1$ level from the lifetime of the level the branching ratio of the level, must be known. The possible transitions from the level are:

$$\begin{aligned} 6s7p\,^1P_1 &\rightarrow 6s^2\,^1S_0 \quad 3072\ \text{Å} \\ &\rightarrow 6s5d\,^1D_2 \quad 4726\ \text{Å} \\ &\rightarrow 5d^2\,^1D_2 \quad 10\,542\ \text{Å} \\ &\rightarrow 6s7s\,^1S_0 \quad (23\,164\ \text{Å}) \\ &\rightarrow 6s5d\,^1D_2 \quad (43\,285\ \text{Å}) \end{aligned}$$

The wavelength in brackets have been calculated from the energy levels given by Moore (1958). These bracketed transitions, because of their long wavelengths, can be neglected. The oscillator strengths of the transitions are given in Table VI.

TABLE VI

Experimental and Theoretical Quantities Relating to the $6s7p\,^1P_1$ State of Barium

Lifetime

Ma et al. (1970)	13.4±0.6	10^{-9} sec
This work	13.2±0.4	

g_J Value

Ma et al. (1970)	1.003(2)

Oscillator Strengths - Experimental

Upper level	$6s6p\,^1P_1$	$6s7p\,^1P_1$	$6s7p\,^1P_1$	Ref.
Lower level	$6s^2\,^1S_0$	$6s^2\,^1S_0$	$6s5d\,^1D_2$	
(Å)	5535	3072	4726	
relative f-value	1000	109	87.6	1,2
absolute f-value	1.59	0.17	0.14	3
		0.19±0.01	0.060±0.004	4
		0.12±0.05	0.09 ±0.04	5

Oscillator Strengths - Theoretical

$6s7p\,^1P_1 \rightarrow 6s^2\,^1S_0$	3072 Å	∿0.22	6
$\rightarrow 6s5d\,^1D_2$	4726 Å	∿0.34	
$\rightarrow 5d^2\,^1D_2$	10542 Å	0.19∿0.66	

Ref. 1 Ostrovskii and Penkin (1960)
2 Penkin and Shabanova (1962)
3 Miles and Wiese (1969)
4 Ma et al. (1970)
5 This work
6 Freidrich and Trefftz (1969)

The ratios of the oscillator strengths of the lines 4726 and 3072 Å to that of 5535 Å are taken from the data of Penkin and Shabanova (1962) and Ostrovskii and Penkin (1960). The recent calculations of Friedrick and Trefftz (1969) indicate that the oscillator strength of the 10 542 Å line is of the same order of magnitude as that of 3072 even though the transition involves two electrons. However, even if the oscillator strength is this large the line would contribute only 15% to the sum of the A coefficients because of its longer wavelength.

This calculated oscillator strength is not reliable, and as the error inherent in the use of the ratio f(3072): f(4726) is probably at least 15% the 10 542 Å line is not included in the calculations.

Using our value for τ, and the ratio f(3072): f(4726) given in the table we find

$$f(3072) = 0.12 \pm 0.05$$

$$f(4726) = 0.09 \pm 0.04$$

where the error is put at about 30% from the uncertainty in the branching ratio. These results for the f values differ from those of Ma et al (1970) because they use a branching ratio calculated from data given in the tables of Corliss and Bozman (1962) who in turn obtain their data from measurements of the relative intensity of spectral lines of small percentages of elements put into a copper arc. The tables of Corliss and Bozman are extensive

but are not reliable, and the uncertainties can be up to 100% and are frequently greater than 50% (see for example Crossley 1969 p. 241). Where alternative data is available it is preferable to use it. Miles and Wiese (1964) state that the data of Penkin and co-workers is the best available and consequently we have used Penkins results.

$5d6p\,^1P_1$

The Hanle resonance of the $5d6p\ ^1P_1$ level was observed using the transition $5d6p\ ^1P_1 - 6s^2\ ^1S_0$, 3501 Å, the geometric arrangement shown in Fig. 11 (iii), and the signal averaging electronics shown in Fig. 9 (ii). The results of 8 determinations of the full width at half height of the resonances are given in Table VII . The weighted mean of the 8 determinations is 9.30 ± 0.07G; from which $g_J\tau = 12.20 \pm 0.1 \times 10^{-9}$ sec. Our result agrees well with that of Ma et al. (1970) who obtained $\tau = 12.40 \pm 0.9 \times 10^{-9}$ sec., and who found $g_J = 1.004 \pm 0.002$.

From our value for the lifetime the absolute oscillator strengths of the transitions from the $5d6p\,^1P_1$ level can be determined from the relative oscillator strengths implicit in the data of Penkin and Shabanova (1962) and Ostrovskii and Penkin (1960). The most important transition, apart from the resonance line $4d6p\,^1P_1 - 6s^2\ ^1S_0$ at 3501 Å, is that to the $5d6s\ ^1D_2$ level at 5826 Å; the ratio of the oscillator strengths

TABLE VII

Experimental Quantities Pertaining to $5d6p\,^1P_1$		
Full width at half intensity of Hanle resonance (the errors are those given by the fitting program).	34.74 ± 0.6 36.26 ± 0.5 36.07 ± 0.7 36.49 ± 0.5 35.66 ± 0.8 36.14 ± 1.1 37.85 ± 1.7 34.60 ± 1.4	
Weighted mean	35.95 ± 0.29 channels	
or	9.30 ± 0.07 Gauss	
Lifetime	$12.22 \pm 0.10 \times 10^{-9}$ sec.	ref c
	$12.4 \pm 0.9 \times 10^{-9}$	e

Oscillator Strengths				Ref.
Upper level	$6s6p\,^1P_1$	$5d6p\,^1P_1$	$5d6p\,^1P_1$	
Lower level	$6s^2\,^1S_0$	$6s^2\,^1S_0$	$6d5s\,^1D_2$	
Wavelength (Å)	5535	3501	5826	
Relative oscillator strengths	1000	102	187	a,b
Absolute oscillator strengths		0.10±0.02	0.19±0.04	c
		0.16	0.30	d
		0.22±0.02	0.12±0.01	e

a Penkin and Shabanova (1962)
b Ostrovskii and Penkin (1960)
c This work
d Miles and Wiese (1969)
e Ma et al (1970)

is f(3501):f(5826) = 102:186, from which the absolute values are obtained as,

$$f(3501) = 0.10 \pm 0.02$$

$$f(5826) = 0.19 \pm 0.04$$

where the errors have been put at about 20% to take account of the probable error in the ratio.

These results are in reasonable agreement with those of Miles and Wiese, but are in poor agreement with those of Ma et al who have used a branching ratio calculated from the data of Corliss and Bozmann as has been discussed for the results of the $6s7p\ ^1P_1$ level; the results are collected in Table VII, while Fig. 15 is a plot of the experimental points and the theoretical fit of a typical resonance.

Fig.15 Hanle effect of $5d6p\ ^1P_1$.

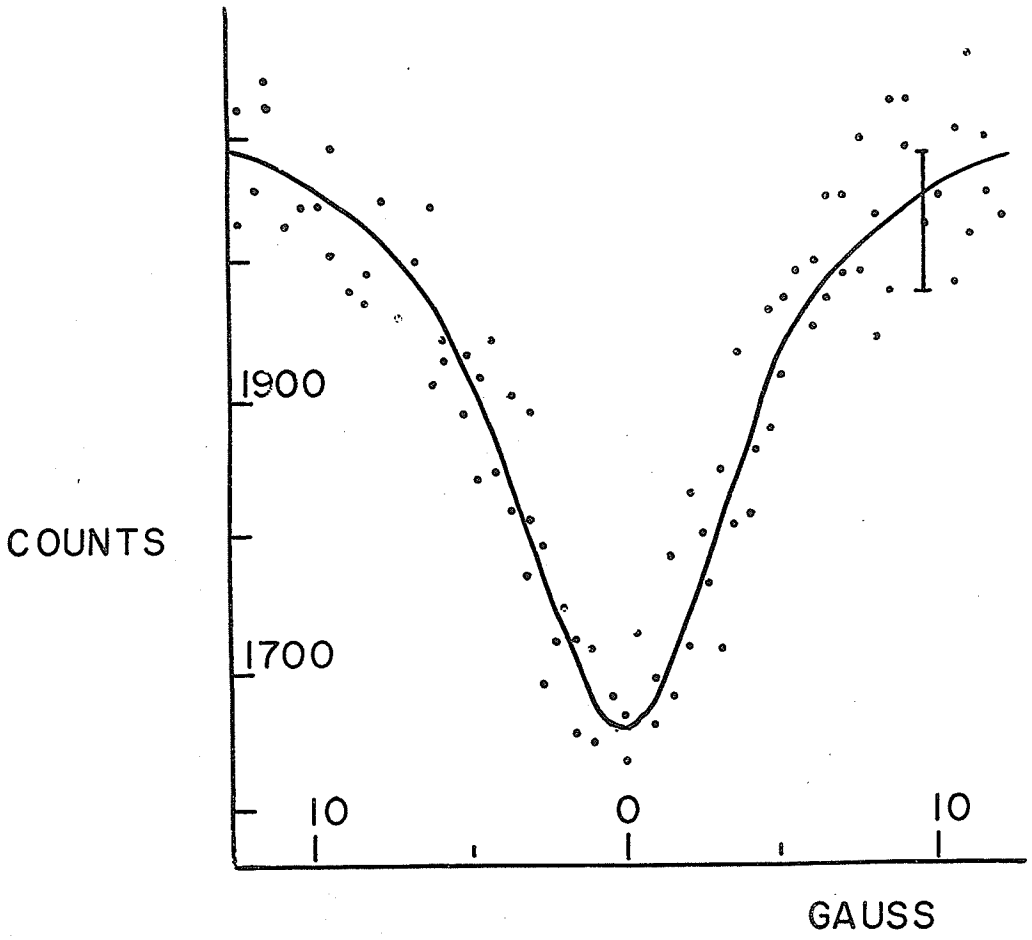
1900
1700
COUNTS
10
0
10
GAUSS

DISCUSSION OF THE RESULTS

The lifetime obtained for the first excited singlet P level agrees well with the results of previous authors, and the results obtained for the 6s7p and 5d6p configurations agree well with the recent, but as yet unpublished, results of Ma, Lido, and zuPutlitz. In all cases the precision of the results is better than that of other authors.

The Hanle resonance of the $6s8p\,^1P_1$, level could not be observed. The oscillator strength of the transition from this level to the ground level $6s^2\,^1S_0$ is small and even though the line could be observed in the spectrum of the hollow cathode lamp - albeit with a very low intensity - no Hanle curves could be obtained. Two changes might make the resonance observable; an increase in beam density and an increase in lamp intensity. With the present apparatus the limit on beam density is set by the distance between the furnace and the scattering region and by the power that can be fed to the furnace. The power is limited by the onset of a discharge in the cloud of barium vapour at the mouth of the furnace while the distance between the furnace and the scattering region could be substantially reduced only by extensive rebuilding

of the beam tube.

At present work is underway to increase the effective f/number of the hollow cathode lamp and to increase the discharge current, at present limited to about 200 mA, to increase the light output from the lamp. More efficient polarizers would also help; at present they absorb almost 85% of the light.

The lifetimes of the levels are of interest because they allow the oscillator strengths of transitions from the levels to be determined and in addition they provide information about the coupling of the valence electrons. The degree of mixing between the wave functions representing the ^1P and ^3P levels is reflected in the lifetimes of the levels and the oscillator strengths of the transitions from these levels to the ground state. In pure LS coupling the intercombination line is forbidden and its presence can be attributed to the mixing of the $^1P_1$ level with the $^3P_1$ level.

The oscillator strengths that can be determined from the lifetimes of the levels depend on earlier determinations of the relative oscillator strengths of the transitions from these levels. This limits the accuracy to about 20 or 30% in most cases and in addition the use of data from different authors can lead to very different results. This lack of precision is typical of the situation in the spectra of many elements and the

lifetimes can point to serious discrepancies in the oscillator strengths.

In the case of the 6s6p and 6s7p $^1P_1$ configurations the lifetime of the first member of the series, 6s6p, together with the branching ratio of the level and the relative oscillator strength of the resonance line from the 6s7p level, allow the oscillator strength of this resonance line to be determined. The oscillator strength of the line can also be found from the lifetime and branching ratio of the level. The results of the two methods of using the data agree and confirm earlier work.

For the 5d6p ^1P level the branching ratio obtained from the data of Penkin and his co-workers is very different to that of Corliss and Bozman; even though the results of Penkin are generally considered more reliable than those of Corliss and Bozman further work to determine which branching ratio is correct is desirable.

A preliminary report of the work on the 6s6p level was presented at the C.A.P. meeting at Waterloo in 1969 (Dickie and Kelly 1969) while a full report appeared in 1970 (Dickie and Kelly 1970). A preliminary report of the 6s7p work was presented at the joint C.A.P. - S.M.F. - A.P.S. meeting in Winnipeg in 1970 (Dickie and Kelly 1970a) while a full report will appear shortly (Dickie and Kelly 1971).

REFERENCES

Arroe,O.H., and Mack,J.E. 1950. J.Opt.Soc.Am. 40,386.

Barrat,J.P. 1957. Compt.Rend. 244,2785.

- 1959. J.Phys.Radium, 20,541,633,657.

Bitter,F. 1949. Phys.Rev. 76,833.

- 1962. Appl.Optics, 1,1.

Breit,G. 1933. Rev.Mod.Phys. 5,71.

- and Wills,L.A. 1933. Phys.Rev. 44,470.

Brossel,J, and Bitter,F. 1952. Phys.Rev. 86,308.

- and Kastler,A. 1949. Compt.Rend. 229,1213.

Bucka,H.,Kopfermann,H., and zuPutlitz,G. 1961. Z.Physik,165,72.

- and Nagel,H.H. 1961. Ann.Physik, 8,329.

- and Schussler,H.J. 1961. Ann.Physik,7,5.

Budick,B. 1967. Advan.At.Mol.Phys. 3,73.

- Novick,R., and Lurio,A. 1965. Appl.Optics, 4,229.

Cario,G., and Lochte-Holtgreven,W. 1927. Z.Physick, 42,22.

Colgrove,F.D.,Franken,P.A.,Lewis,R.R., and Sands,R.H. 1959. Phys.Rev.Lett. 3,420.

Condon,E.U., and Shortly,G.H.. 1963. The theory of atomic spectra (Cambridge University Press,London).

Crossley,R.J.S. 1969. Advan.At.Mol.Phys. 5,237.

Davydov,A.S. 1965. Quantum mechanics (Pergamon Press,Oxford).

Dickie,L.O., and Kelly,F.M. 1969. Phys. in Can. 25,No.4,41.

- 1970. Can.J.Phys. 48,879.

- 1970a. Phys. in Can. 26,No.4,65., and Bull.Am.Phys.Soc. 15,795.

- 1971. Can.J.Phys. in press.

Fisher,W., and Huhnermann,H. 1969. J.Phys.(France), 30,C1-59.

Foster,E.W. 1964. Repts.Prog.Phys. 27,469.

Franken,P.A. 1961. Phys.Rev. 121,508.

- 1969 Atomic Physics. ed.Bederson,B.(Plenum Press, New york)

Freidrich,H., and Trefftz,E. 1969. J.Quant.Spectrosc.Radiat. Transfer. 9,333.

Fry,E.S., and Williams,W.L. 1969. Phys.Rev. 183,81.

Gotmeister,V.P. 1968. Optics Spectrosc. 25,185.

Handrich,E.,Steudel,A.,Wallstein,R., and Walter,H. 1969. J.Phys.(France),30,C1-18.

Hanle,W. 1924. Z.Physik, 30,93.

Happer,W. 1968. Beam-foil spectroscopy. ed.Bashkin,S.(Gordon and Breach,New York).

Heitler,W.1954. The quantum theory of radiation (Oxford University Press,London).

Holstein,T. 1947. Phys.Rev. 72,1212.

1951. Phys.Rev. 83,1159.

Hulpke,E.,Paul,E., and Paul,W. 1964. Z.Physik, 177,257.

Jackson,D.A., and Duong,H.T. 1964. Proc.Roy.Soc. (London),A280,323.

– 1966. Proc.Roy.Soc.(London),A291,9.

Kelly,F.M., and Tomchuk,E. 1964.Can.J.Phys. 42,918.

Landman,D.A. 1968. Phys.Rev. 173,33.

Lurio,A. 1964. Phys.Rev. 136,A376.

– 1966. Phys.Rev. 142,46.

– Mandl,M., and Novick,R. 1962. Phys.Rev. 126,1785.

– deZafra,R.L., and Goshen,R.J. 1964. Phys.Rev. 134,1198.

Ma,I.J.,Lido,G., and zuPutlitz,G. 1970.private communication.

Miles,B.M., and Wiese,W.L. 1969. Washington,D.C.,Technical Note 474. National Bureau of Standards.

Mitchell,A.C.G., and Zemansky,F.W. 1934.Resonance radiation and excited atoms (Cambridge University Press,London).

Moore,C.E. 1958. Atomic energy levels.Washington,D.C.,Circular 467.National Bureau of Standards.

Ostrovskii,Yu.I., and Penkin,N.P. 1960. Optics Spectrosc. 9,371.

– Penkin,N.P., and Shabanova,L.N. 1958. Sov.Phys.-
-Dokaldy,3,538.

Penkin,N.P., and Shabanova,L.N. 1962. Optics Spectrosc. 12,1.

Piper,J.A., and Sandle,W.J. 1970. J.Phys.B:Atom.Molec.Phys. 3,1357.

Pryce,M.H.L. 1950. Phys.Rev. 77,136.

zuPutlitz,G. 1963. Ann.Physik, 11,248.

– 1965. Ergebnisse der exakten Naturwissenschaften,
37,105 (Springer-Verlag,Berlin).

– 1969. Atomic physics. ed.Bederson,B.(Plenum Press,
New York).

Saloman,E.B., and Happer,W. 1966. Phys.Rev. 144,7.

Rose,M.E., and Carovillano,R.L. 1961 Phys.Rev. 122,1185.

Russell,H.N., and Moore,C.E. 1955. J.Res.Natl.Bur.Std.(U.S.A.)
55,299.

Sawyer,R.A. 1930. Phys.Rev. 36,44.

Schuler ,H. 1926. Z.Physik, 35,323;ibid 59,149 (1930).

Series,G. 1959. Repts.Prog.Phys. 22,280.

– 1969. Physics of the one and two electron atoms ed.Bopp,F. and Kleinpoppen,H.(North Holland,Amsterdam).

Stroke,H.H.,Fulop,G.,Klepner,S., and Redi,O. 1968. Phys.Rev.Lett. 21,61.

Swagel,M.W., and Lurio,A. 1968. Phys.Rev. 169,114.

Tolansky,S. 1947. High resolution spectroscopy (Methuen,London).

Van Heel,A.C.S. 1967. ed, Proc.Zeeman centenial conference, Physica 33.

Weisskopf,V. 1931. Ann.Physik, 9,23.

Wessel,G.1949. Z.Physik, 126,440.

– 1951. Z.Physik, 130,106.

Wiese,W.L. 1968. Methods Exptl.Phys. 7A,117;7B,307.

Wood,R.W. 1905.Phil.Mag. 10,513.

- and Ellet,A. 1924. Phys.Rev. 24,243.

d'Yakanov,M.I., and Perel',V.I. 1965. Sov.Phys.-JETP,20,997.

deZafra,R.L., and Kirk,W. 1967. Am.J.Phys. 35,573.

Zeeman.P. 1897. Phil.Mag. 44,255.

supplementary references:

Dicke, R. H., and Wittke, J. P. 1960. Introduction to

- Quantum Mechanics (Addison - Wesley, Reading)

Happer, W., and Saloman, E. B. 1967. Phys. Rev. Lett. 15, 441.

Lifetime of the $6s6p\ ^1P_1$ level of barium

L. O. DICKIE AND F. M. KELLY
Department of Physics, University of Manitoba, Winnipeg, Manitoba

Received November 17, 1969

The lifetime of the first excited singlet P level of barium, $6s6p\ ^1P_1$, has been determined from the width of the zero field level crossing, i.e. the Hanle effect, of the $6s6p\ ^1P_1 - 6s^2\ ^1S_0$, 5535 Å resonance line. The resonance radiation was produced in a hollow cathode lamp and the scattering atoms by an atomic beam. After taking account of coherence narrowing, the lifetime is determined to be $8.37 \pm 0.14 \times 10^{-9}$ s, in good agreement with other recent work.

Canadian Journal of Physics, 48, 879 (1970)

The energy levels of an atom which is placed in a magnetic field are split into the well-known Zeeman states. If fine or hyperfine structure is present there is a possibility of two of the Zeeman states crossing at a nonzero magnetic field. When polarized resonance radiation is scattered from such a system, the spatial distribution of the scattered radiation is changed as the energy levels cross. Such level crossings have become important in atomic spectroscopy (Colegrove *et al.* 1959; Budick 1967). As the magnetic field is reduced the separations of the various Zeeman states become smaller, and at zero field the Zeeman states become degenerate. At this zero field level crossing there is also a spatial redistribution of scattered resonance radiation. Hanle (1924) was the first to give a theoretical explanation, based on the Zeeman effect of this zero field level crossing, now called the Hanle effect.

The width of an energy level is inversely proportional to the lifetime of the level. Consequently, level crossings of Zeeman states take place over a range of magnetic field, and the width of the observed resonance, measured in terms of the magnetic field, depends on the lifetime of the level, and the Hanle effect becomes a convenient method for determining lifetimes of excited atomic levels. The early work on the Hanle effect is discussed by Mitchell and Zemansky (1934) and the general theory of the scattering of resonance radiation was developed by Weisskopf (1931) and Breit (1933). More recently the theory has been put into forms more directly useful for atomic spectroscopy by Rose and Carovillano (1961), Franken (1961), and Lurio, deZafra, and Goshen (1964).

The geometry used in our Hanle experiment is shown in Fig. 1. The magnetic field is in the z direction. The input light is directed along the x direction and is plane polarized with the electric vector along the y axis; the output light is observed along the y axis. In the experiments discussed, the transitions are between an excited $^1P_1$ level and a ground $^1S_0$ level, and for even isotopes, for which the spin is zero, the Hanle signal intensity can be written as

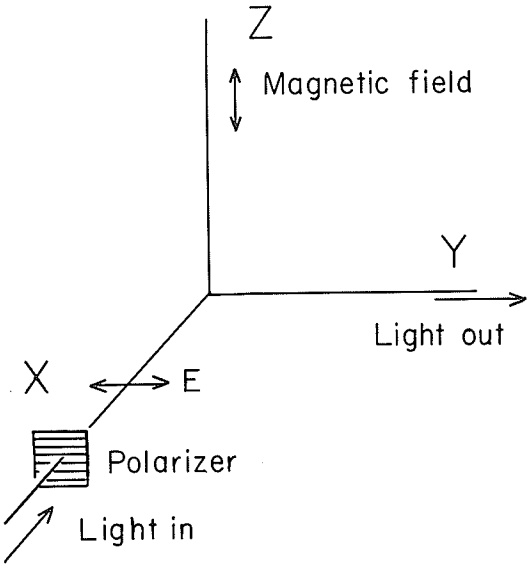

FIG. 1. Geometry of this Hanle experiment.

$$I = I_0\left[1 - \frac{1}{1 + (2g_J\mu_0 H\tau/\hbar)^2}\right]$$

where g_J is the g value of the $^1P_1$ state, μ_0 is the bohr magneton, and I_0 is proportional to both the number of scattering atoms and the intensity of the exciting light.

The full width at half intensity, ΔH, of the resonance is related to the lifetime, τ, by

$$\frac{1}{\tau} = \frac{g_J\mu_0}{\hbar}\Delta H$$

Ideally the shape of the resonance is Lorentzian. However, if the angle between the incident and observing directions is not exactly 90°, the curve is a combination of a Lorentzian and a dispersion curve. As well, the exciting light and the observed light are averaged over small solid angles about the ideal directions. Both of these effects are discussed by Fry and Williams (1969).

A major advantage of the Hanle method is that at low densities of scattering atoms, the width of the resonance is independent of the density so that an absolute value of the density is not required. At higher densities the width of the Hanle resonance curve is decreased by coherence narrowing. This effect has been studied theoretically by Barrat (1959) and d'Yakonov and Perel (1964, 1965) and the theory has been compared with experiment by Barrat (1959) and by Happer and Saloman (1967).

In contrast, both the 'hook' method and absorption methods for determining absolute oscillator strengths require a value of the density. The density of scattering atoms is difficult to measure and, as a consequence, some oscillator strengths determined by these methods have large and unknown systematic errors.

The $6s6p\ ^1P_1$ level of barium can decay directly to the ground state $6s^2\ ^1S_0$ by emission of a photon of the resonance line 5535 Å, and also to the metastable level $6s5d\ ^1D_2$ with a photon of wavelength 15 000 Å. These levels of barium are shown in Fig. 2. The lifetime of the $^1P_1$ level depends on the oscillator strengths of both transitions. However, the infrared line is much weaker than 5535, as the oscillator strengths are in the ratio 1.5:0.10, using the values given

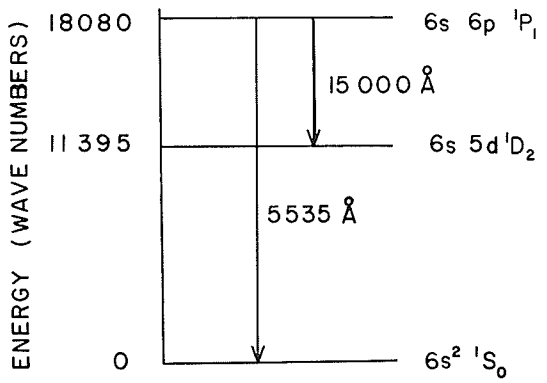

FIG. 2. Relevant energy levels and transitions of barium.

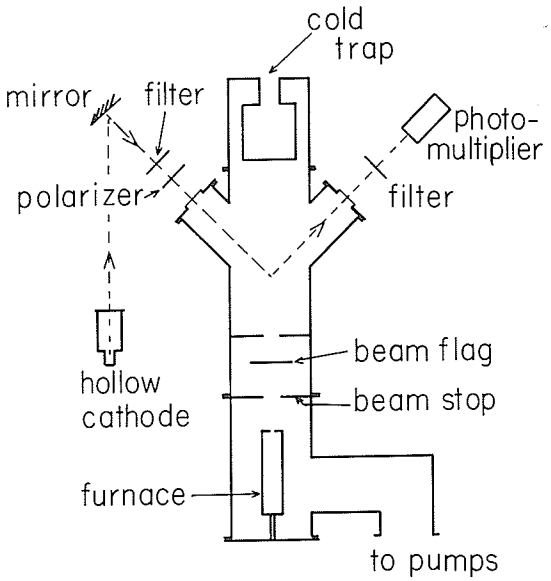

FIG. 3. Schematic diagram of the experimental apparatus; the static magnetic field is perpendicular to the plane of the diagram.

by Miles and Wiese (1969). Thus the effect of the infrared transition on the lifetime of the $6s6p\ ^1P_1$ level can be neglected.

A schematic diagram of our experimental apparatus is given in Fig. 3. The light from the hollow cathode lamp is focussed onto a beam of barium atoms. The light is linearly polarized in the plane containing the light input and output directions (and the beam), with the electric vector perpendicular to the direction of the static magnetic field. An interference filter is used to isolate the required line in each of the input and output arms.

The beam of barium atoms is produced in an electrically heated oven. The beam is collimated by beam stops and a beam flag can be used to cut off the beam. The chamber is blackened and baffled to reduce the scattered light. Natural barium, 82.1% even isotopes and 17.9% odd isotopes, is used in the experiment. Both odd isotopes have spin 3/2.

After passing the scattering region, the atomic beam is stopped by a liquid nitrogen cooled trap. The trap also helps to keep the pressure low. The residual gas pressure inside the chamber is about 10^{-5} mm Hg when the beam is operating.

The light scattered from the beam in a direction perpendicular to both the incident light and

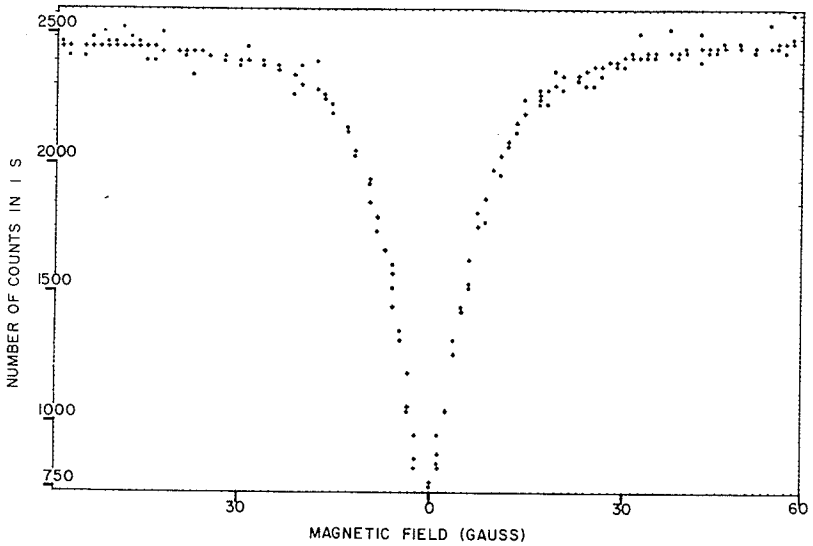

FIG. 4. Typical plot of the experimental and theoretical counts vs. magnetic field; the dots are the experimental points, the crosses theoretical.

the magnetic field is focussed on to an EMI type 6256 photomultiplier. The photomultiplier is some distance from the scattering region and is surrounded by μ metal to shield it from the magnetic field. Initially the DC output from the photomultiplier was monitored and a lock-in amplifier was used to determine the shape of the resonance curve. However, light intensities are low and small beam densities are used so that photon counting became a preferable experimental arrangement. As well, this change eliminates corrections which must be applied for the strength of the lock-in oscillating magnetic field and for the integrating time of the lock-in amplifier. For photon counting the signal from the photomultiplier is amplified, passed into a discriminator to eliminate low-noise events, and the output fed into a scalar.

The magnetic field is supplied by a pair of Helmholtz coils, 40 cm in diameter. The coils were calibrated using a Rawson–Lush rotating coil gaussmeter, and were adjusted until the field at the scattering region was constant to better than one part in 10 000 over a cube of side 2 cm. The current in the coils was monitored by measuring the voltage across a 1 Ω standard resistor with a digital voltmeter. The field was found to depend linearly on the current over the range tested, 0–300 G.

The shape of our experimental curves is found by plotting the number of photons scattered into the photomultiplier in a fixed period against the magnetic field. The counting periods were made long enough to give good statistics and were between 1 and 10 s.

A typical run is made by varying the magnetic field in steps from about −60 G through zero to +60 G, and involves between 60 and 100 points, while the output of the hollow cathode and the beam density are kept fixed. It requires between 5 and 10 min to accumulate this data. The light output from the hollow cathode could be kept constant for this period of time but difficulties were experienced with gradual changes of the beam density.

The data is analyzed by a computer program that fits a Lorentzian to the experimental points and gives the full width at half intensity and other parameters of the best fit. The program also plots a graph of the experimental and theoretical counts.

Figure 4 is a typical graph of the experimental and theoretical counts versus magnetic field. Because the program fitted a Lorentzian to the experimental points, the difference between the calculated and experimental counts was plotted to check whether any dispersive component was present. Such a component can arise from a departure of the scattering angle from 90° or from misalignment of the polarizer (Fry and Williams 1969; Stroke *et al.* 1968). Great care was taken in aligning the apparatus and the solid

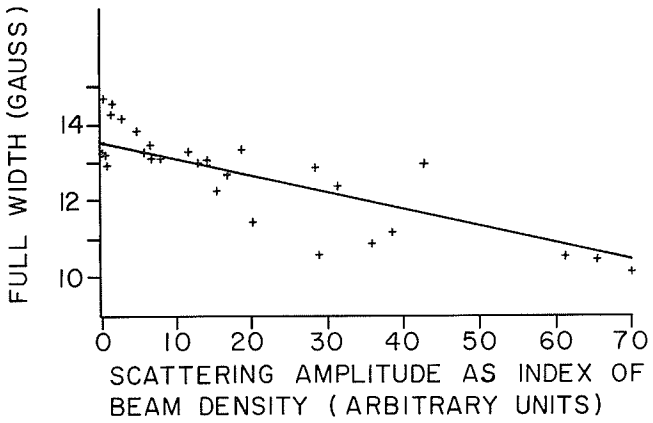

FIG. 5. Dependence of the full width at half maximum on scattering atom density.

angle from which scattered radiation was accepted was kept small. A few of the curves obtained at higher beam densities showed small dispersive components and were not used in obtaining the final result. Other curves, also at higher beam densities, showed symmetrical departures from the ideal shape.

The presence of 17.9% odd isotopes in the natural barium might be expected to affect the shape of the resonance curve. However, Lurio (1964) carried out a similar experiment using separated even isotopes and found no difference from the results given by natural barium.

No attempt was made to measure the density of the scattering atoms in the atomic beam, so the contribution of coherence narrowing to the line width could not be directly calculated. Instead, a series of measurements at different densities was made and the true width found by extrapolating to zero density. The amplitude of the Lorentz peak is used as a parameter proportional to density. The dependence of the full width at half intensity of the resonance on this parameter is shown in Fig. 5.

The amplitude of the Lorentz peak is one of the parameters given by the computer fit. Theoretically, this is proportional to both the number of scattering atoms and to the intensity of the incident light (Franken 1961). We have used this amplitude, normalized to constant intensity of the input light, as an index of beam density. For low densities where multiple scattering effects are not important, this amplitude is a reliable indication of beam density.

Coherence-narrowing theory predicts that the true half-width Γ is related to the measured half-width Γ_2 by $\Gamma/\Gamma_2 = 1 - A_2 x$ (d'Yakonov and Perel 1964, 1965).

For the two levels $^1S_0$ and $^1P_1$, A_2 is 0.7 and x depends on the length of the scattering region, the density of the scattering atoms, and on the lifetime of the excited level; values are tabulated by Mitchell and Zemansky (1934). The length of the scattering region is about 2 cm but we have an index proportional to the scattering atom density rather than the absolute density. However, at low densities x is small and changes very slowly as the atom density changes over several orders of magnitude, so that the theoretical relationship between the experimental half-width and density can be approximated by a straight line.

A least-squares fit to a straight line of the 32 experimental determinations of the width of the resonance gives the full width at zero beam density as 13.58 ± 0.21 G. The error quoted is obtained by combining the standard deviation of the intercept with the axis and the uncertainty in the calibration and measurement of the magnetic field. Then, to take account of unknown systematic errors and the approximation involved in the straight-line extrapolation, we multiply by 5 to give a total error of 1.6%.

At the highest density of scattering atoms shown in Fig. 5, the ratio of measured width to the zero-density width is 10.27:13.58 or 0.76:1. If we substitute this ratio into the coherence-narrowing formula using our previous estimate of 2 cm for the size of the scattering region, and a preliminary figure of 8.3×10^{-9} s for the lifetime

of the level, the density of the scattering atoms is about 5×10^9 atoms cm^{-3}. It is at about this density that the shape of the coherence-narrowing curve begins to depart significantly from a straight line. If we omit the last three points shown in the graph from the least-squares calculation, the zero intercept is reduced slightly to 13.52 ± 0.21 G, while both the calculated density and the value of the index of beam density are reduced by about one half at the highest density used. At this density the approximations involved in making the straight-line extrapolation and in using the amplitude of the Lorentz peak as an index of beam density are valid. At the lowest beam densities used the count rates are low and the statistics are poor, resulting in a rather large scatter of the experimental points. For this reason a least-squares fit to a straight line over a range of densities gives a more reliable value.

The two values for the intercept of the straight-line extrapolation with the zero-density line agree within our estimated errors, and using the smaller value and $g_J(^1P_1) = 1.0039$ (Swagel and Lurio 1968), we obtain $\tau = 8.37 \pm 0.14 \times 10^{-9}$ s. The two most recent determinations of the lifetime of the $^1P_1$ state are those of Hulpke, Paul, and Paul (1964), who used the phase-shift technique, and Lurio (Swagel and Lurio 1968), who used the Hanle effect. These results together with that of this work are given in Table I. The agreement between the results is very good. The oscillator strength of the transitions is given by Swagel and Lurio (1968) and by Miles and Wiese (1969) in the recent survey of the barium transition probabilities.

TABLE 1

Lifetime of $^1P_1$ of Ba

Swagel and Lurio (1968)	8.37 ± 0.20 ns
Hulpke *et al.* (1964)	8.36 ± 0.25 ns
This work	8.37 ± 0.14 ns

Acknowledgment

This research was supported by a grant from the National Research Council of Canada.

BARRAT, J. P. 1959. J. Phys. Radium, **20**, 541, 633, 657.
BREIT, G. 1933. Rev. Mod. Phys. **5**, 91.
BUDICK, B. 1967. Advan. At. Mol. Phys. **3**, 73.
COLEGROVE, F. D., FRANKEN, P. S. S., LEWIS, R. R., and SANDS, R. H. 1959. Phys. Rev. Lett. **3**, 420.
FRANKEN, P. A. 1961. Phys. Rev. **121**, 508.
FRY, E. S. and WILLIAMS, W. L. 1969. Phys. Rev. **183**, 81.
HANLE, W. 1924. Z. Physik, **30**, 93.
HAPPER, W. and SALOMAN, E. B. 1967. Phys. Rev. **160**, 23.
HULPKE, E., PAUL, E., and PAUL, W. 1964. Z. Physik, **177**, 257.
LURIO, A. 1964. Phys. Rev. **135**, 376.
LURIO, A., DEZAFRA, R. L., and GOSHEN, R. J. 1964. Phys. Rev. **134**, 1198.
MILES, B. M. and WIESE, W. L. 1969. Washington, D.C., Technical Note 474. National Bureau of Standards.
MITCHELL, A. C. G. and ZEMANSKY, M. W. 1934. Resonance radiation and excited atoms (Cambridge University Press, London).
ROSE, M. E. and CAROVILLANO, R. L. 1961. Phys. Rev. **122**, 1185.
STROKE, H. H., FULOP, G., KLEPNER, S., and REDI, O. 1968. Phys. Rev. Lett. **21**, 61.
SWAGEL, M. W. and LURIO, A. 1968. Phys. Rev. **169**, 114.
WEISSKOPF, V. 1931. Ann. Physik, **9**, 23.
D'YAKONOV, M. I. and PEREL, V. I. 1964. J. Exp. Theoret. Phys. (U.S.S.R.) **47**, 1483.
——— 1965. Sov. Phys.–JETP, **20**, 997.

Lifetime of the $6s7p^1P_1$ Level of Barium

L. O. DICKIE AND F. M. KELLY
Department of Physics, University of Manitoba, Winnipeg, Manitoba
Received November 25, 1970

The lifetime of the second excited singlet P level of barium $6s7p^1P_1$ has been determined from the width of the Hanle resonance of the $6s7p^1P_1$–$6s^2\ ^1S_0$ 3071.58 Å resonance line. The lifetime is determined to be $13.2 \pm 0.4 \times 10^{-9}$ s. From this lifetime the oscillator strength of the 3072 Å transition is 0.12 ± 0.05 and that of the $6s7p^1P_1$–$6s5d^1D_2$, 4726 Å is 0.09 ± 0.04.

La vie moyenne du second niveau excité singulet P du baryum $6s7p^1P_1$ a été déterminée à partir de la largeur de la résonance de Hanle de la ligne résonante $6s7p^1P_1$–$6s^2\ ^1S_0$ 3071.58 Å. Le temps de vie est évalué à $13.2 \pm 0.4 \times 10^{-9}$ s. A partir de ce temps de vie la force d'oscillateur de la transition à 3072 Å est 0.12 ± 0.05 et celle de la transition $6s7p^1P_1$–$6s5d^1D_2$, 4726 Å est 0.09 ± 0.04.

Canadian Journal of Physics, 49, 1098 (1971)

The zero field level crossing, or Hanle effect, is a convenient method for measuring the lifetimes of excited atomic levels, particularly those levels that can be populated by optical excitation from the ground state. The theory of the Hanle effect has been discussed by Lurio, de Zafra, and Goshen (1964), while Budick (1967) has reviewed level crossing methods in general. In our experiments, which have been described previously (Dickie and Kelly 1969), barium resonance radiation is incident on an atomic beam of barium atoms. The light scattered at 90° to both the direction of the incident light and the direction of the magnetic field is detected by a photomultiplier as shown in Fig. 1.

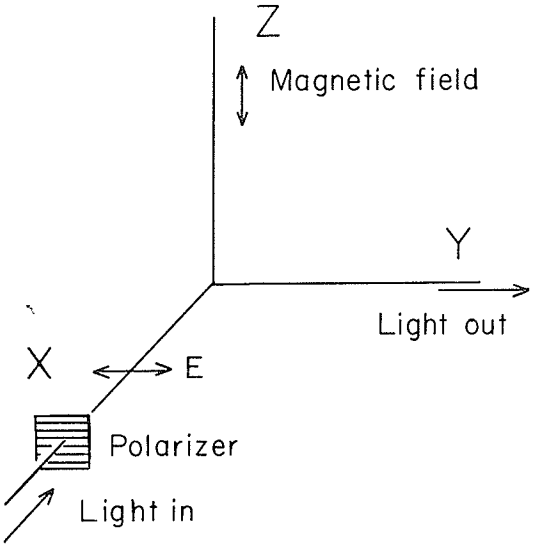

FIG. 1. Geometry of the Hanle experiment.

In this paper we report on an experiment to determine the lifetime of the $6s7p^1P_1$ level of barium from a measurement of the full width at half-height of the Hanle resonance in the transition $6s^2\ ^1S_0$–$6s7p^1P_1$ 3071.58 Å. A partial energy level diagram of barium is shown in Fig. 2.

The resonance radiation is produced in a hollow cathode lamp cooled by an ice–water bath. The current in the hollow cathode is controlled by a constant current supply. The intensity of the lines of interest is sufficiently constant that a separate photomultiplier system to monitor the lamp intensity is not necessary.

The light is linearly polarized by a polaroid filter type HNP'B so that the electric vector is

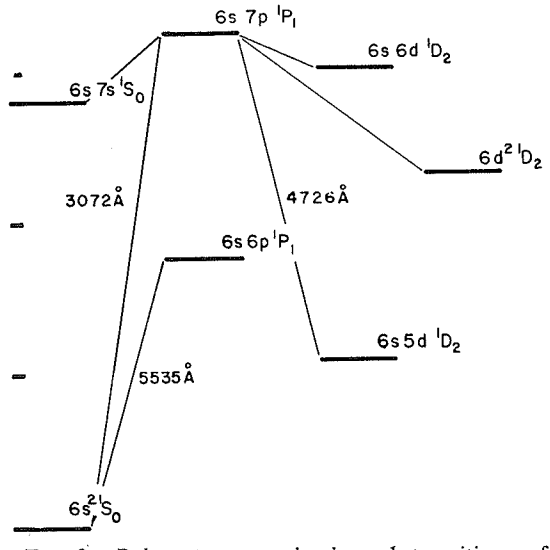

FIG. 2. Relevant energy levels and transitions of barium.

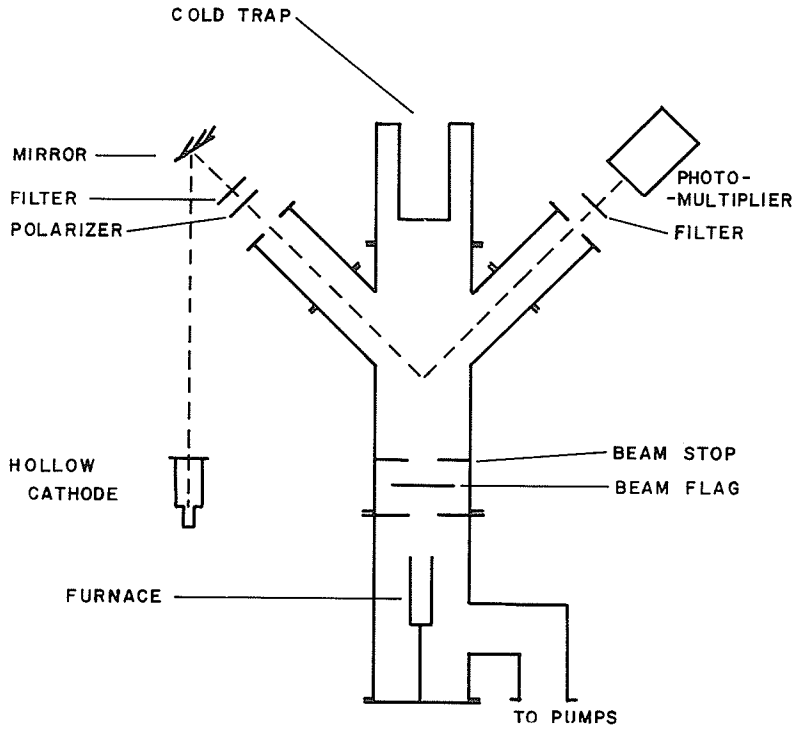

FIG. 3. Schematic diagram of the experimental apparatus; the static magnetic field is perpendicular to the plane of the diagram.

perpendicular to the direction of the static magnetic field and in the plane of the input and output directions. An interference filter in the output arm and either an interference filter or a broad band ultraviolet filter in the input arm isolates the required line.

The atomic beam is produced in a d.c. electrically heated oven with a bifilar winding which reduces stray magnetic fields. Natural barium with 82.1 % even isotopes and 17.9 % odd isotopes is used. After the beam passes the scattering region it condenses on a liquid nitrogen cooled cold trap. With the beam operating, the residual gas pressure in the scattering chamber is about 10^{-5} mm Hg. An outline of the experimental apparatus is given in Fig. 3.

The static magnetic field is supplied by a pair of Helmholtz coils 40 cm in diameter; the current field relationship of the coils was determined using a Rawson–Lush rotating coil gaussmeter and during the experimental runs the current passing through a standard resistor in an oil bath is monitored. Two sets of Helmholtz coils set perpendicular to one another cancel the earth's field in directions other than that of the applied static field. To scan across the Hanle resonance another set of Helmholtz coils, concentric with the main coils, is used to apply a symmetric sawtooth ramp field to the scattering region.

Single photon pulses from the EMI6256 photomultiplier are amplified, passed through a single channel amplifier to isolate the single photon peak, then fed into the coincidence input of a Northern Scientific NS606 multichannel analyzer. The magnetic field controls the address of the analyzer. The voltage across a standard resistor in series with the ramp coils is applied to the direct input of the ADC of the analyzer. A photon pulse arriving at the coincidence input causes the analyzer to sample the voltage on the direct input and store the count in an appropriate channel. The standard resistor is immersed in an oilbath which was in turn kept at a constant temperature by an ice–water bath to avoid change in resistance with heating of the resistor. The period of the ramp can be set at 1, 3, or 6 s and runs at each of these were made. A schematic diagram of the signal averaging layout is shown

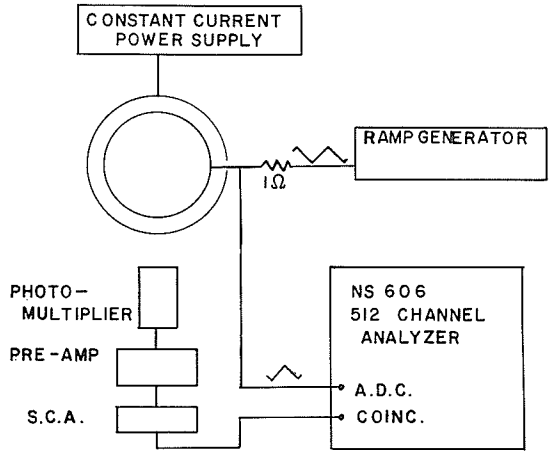

FIG. 4. Schematic diagram of the signal averaging apparatus.

in Fig. 4. Because the count rate of the Hanle peak is different from that in the wings of the resonance, the count rate is kept low enough to ensure that the dead time of the analyzer is not important.

It required runs of between one-half to a few hours to accumulate sufficient counts to give adequate statistics. The oscillator strength of the 3072 Å transition is small and no evidence of coherence narrowing was seen even at the highest beam densities used. Runs were made with different beam densities, different lamp intensities, and different sweep periods. No systematic trends were observed. Each sweep of the magnetic field through the Hanle resonance takes only a few seconds; consequently, slow drifts in the lamp intensity and in the beam density do not enter our results.

The experimental counts were fitted to a Lorentzian and the difference between the calculated and experimental counts plotted to determine whether there was any dispersive component present. A dispersive component can be due to departure of the scattering angle from 90°, or from the use of too large a solid angle in the input or output arms. These effects have been discussed by Fry and Williams (1969). None was observed in our experiments.

Figure 5 is a plot of the experimental counts, and the fitted Lorentzian, against the magnetic field. The error bar shown is plus and minus the square root of the number of counts.

The mean of 14 determinations of the full width at half-height of the Hanle resonance is 8.59 ± 0.25 G; this leads to $g_J\tau(6s7p\,^1P_1) = 13.2 \pm 0.4 \times 10^{-9}$ s. As this work was being completed we learned of the results of Zu Putlitz and co-workers who have carried out a similar experiment and find $\tau = 13.4(6) \times 10^{-9}$ s and who have measured $g_J(6s7p\,^1P_1) = 1.003(2)$.

From our value of the lifetime the oscillator strengths of the transitions from the level can be calculated. The mean life, τ, of the state m is given by

$$\frac{1}{\tau} = \sum_n A_n^m$$

and the Einstein A coefficient, A_n^m, for spontaneous emission from the state m to the lower state n is given by

$$A_n^m = \frac{8\pi^2 e^2}{mc} \frac{g_n}{g_m} \frac{f_n}{(\lambda_{nm})^2}$$

where the g's are the statistical weights of the states and f_n is the absorption oscillator strength for the transition of wavelength λ_{nm} (Mitchell and Zemansky 1934; Crossley 1969).

To obtain the oscillator strengths of the transitions from the $6s7p\,^1P_1$ level from the lifetime of the level, the branching ratio, or ratios of the absorption oscillator strengths of the transitions from the level, must be known. Miles and Weise (1969) have critically compared the available data and suggest that the results of Penkin and Shabanova (1962) and Ostrovskii and Penkin (1960) are the most reliable. These results were obtained with the "hook" method and while this is not accurate for absolute measurements it should give reliable results for the ratios; Miles and Weise estimate that the overall uncertainties are less than 50%. There is in addition the recent theoretical work of Friedrich and Trefftz (1969).

From the data of Penkin and Shabanova and of Ostrovskii and Penkin the ratio of the osillator strengths of the two most important transitions for our consideration is $f(3072):f(4726) = 109:87.6$.

Using our value for the lifetime, and, using only 3072 Å and 4726 Å in the sum of the A's, we obtain $f(3072) = 0.12 \pm 0.05$ and $f(4726) = 0.09 \pm 0.04$. No experimental measurement of the oscillator strength of the transition $6s7p\,^1P_1$–$5d^2\,^1D_2$, 10 542 Å is available.

However, the calculations of Friedrich and Trefftz indicate that the oscillator strength of this transition is of the same order of magnitude as that of 3072, even though the transition involves

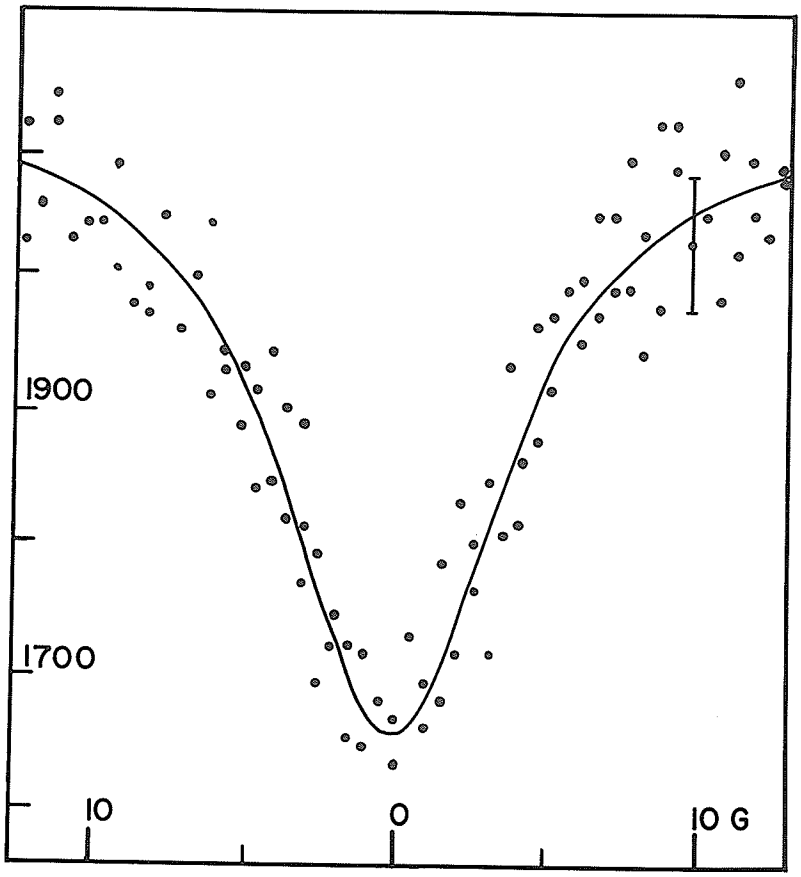

FIG. 5. A plot of the experimental counts, and the fitted Lorentzian, against magnetic field.

TABLE 1. Oscillator strengths of barium lines

				Reference*
Upper level	$6s6p\,^1P_1$	$6s7p\,^1P_1$	$6s7p\,^1P_1$	
Lower level	$-6s^2\,^1S_0$	$-6s^2\,^1S_0$	$-6s5d\,^1D_2$	
λ (Å)	5535	3072	4726	
Relative oscillator strengths	1000	109	87.6	1, 2
Absolute oscillator strengths	1.59	0.17	0.14	3
		0.19 ± 0.01	0.060 ± 0.004	4
		0.12 ± 0.05	0.09 ± 0.04	5

*1, Ostrovskii and Penkin (1960); 2, Penkin and Shabanova (1964); 3, Miles and Weise (1969); 4, Zu Putlitz (1970); 5, This work.

two electrons. If we use this estimate of the f value, the 10 542 Å line contributes only 15% to the sum of the A values, because of its long wavelength.

We have not included 10 542 Å because the calculated f value is not reliable, and the error inherent in the use of the ratio $f(3072):f(4726)$ is greater than 15%. We have estimated the errors at almost 30%. Our agreement with the results obtained using the value $f(5535) = 1.59$ and the ratio $f(5535):f(3072):f(4726)$ is reasonable, as is our agreement with the results of Zu Putlitz (1970), who obtained the branching ratio from the results of Corliss and Bozman (1962).

The differences between our results and those of Zu Putlitz arise from the different branching

ratios used. Neither the branching ratio obtained from the relative f values of Penkin and Shabanova and of Ostrovskii and Penkin nor those from the extensive tables of oscillator strengths of Corliss and Bozman are very reliable. The uncertainties in the results of Corliss and Bozman can be up to 100% (see, for example, Crossley 1969, p. 241), and we prefer to follow Miles and Weise and use the results of Penkin and coworkers.

The results are summarized in Table 1.

A preliminary report of this work was presented at the Joint C.A.P.–A.P.A.–S.M.F. Meeting (Bull. Amer. Phys. Soc. **15**, 795 (1970)).

Acknowledgment

This work was supported by a grant from the National Research Council of Canada.

BUDICK, B. 1967. At. Mol. Phys. **3**, 73.
CORLISS, C. H. and BOZMAN, W. R. 1962. U.S. Nat. Bur. Stand. Monograph 53.
CROSSLEY, R. J. S. 1969. Advan. At. Mol. Phys. **5**, 237.
DICKIE, L. O. and KELLY, F. M. 1969. Can. J. Phys. **48**, 879.
FRIEDRICH, H. and TREFFTZ, E. 1969. J. Quant. Spectrosc. Radiat. Transfer, **9**, 333.
FRY, E. S. and WILLIAMS, W. L. 1969. Phys. Rev. **183**, 81.
LURIO, A., DE ZAFRA, R. L., and GOSHEN, R. J. 1964. Phys. Rev. **134**, 1198.
MILES, B. M. and WIESE, W. L. 1969. U.S. Nat. Bur. Stand. Technical Note 474.
MITCHELL, A. and ZEMANSKY, M. W. 1934. Resonance radiation and excited atoms (Cambridge University Press, London).
OSTROVSKII, YU. I. and PENKIN, N. P. 1960. Opt. Spectrosc. **9**, 371.
PENKIN, N. P. and SHABANOVA, L. N. 1962. Opt. Spectrosc. **12**, 1.
ZU PUTLITZ, G. 1970. Private communication.